

IMPACT OF FAULT STRUCTURES ON THE OCCURRENCE OF GROUNDWATER IN FRACTURED ROCK AQUIFERS

Report to the
Water Research Commission

by

L Lin¹, H Lin¹, Y Xu², T Ntuli¹ and F Mahlangu¹

¹ Council for Geoscience

² Department of Earth Sciences, University of the Western Cape

**WRC Report No 2053/1/14
ISBN 978-1-4312-0641-4**

February 2015

Obtainable from

Water Research Commission
Private Bag X03
GEZINA, 0031

orders@wrc.org.za or download from www.wrc.org.za

DISCLAIMER

This report has been reviewed by the Water Research Commission (WRC) and approved for publication. Approval does not signify that the contents necessarily reflect the views and policies of the WRC nor does mention of trade names or commercial products constitute endorsement or recommendation for use.

EXECUTIVE SUMMARY

Faults are one of the most important geological structures that control the occurrence of groundwater due to their unique fault zone fabrics that differ from the country rock. In hard rock terranes, a fault zone has long been the key locality for groundwater exploration and exploitation owing to the highly fractured zone and dense secondary porosity compared with the country rock. Although this geological structure is conventionally classified into normal, thrust and shear faults, based on relative movement of both walls, in geological history the type of a fault might change over time owing to the change of the crustal driving force. As a result, strata and rocks might be reconstructed by various phases of crustal movement which created different types of discontinuities in the form of joints, faults and unconformities.

Hypothesis

In South Africa, there are more than ten thousand faults recorded in the Geoline Database, whereas very few of them have been investigated and documented. These faults have experienced multiple stages of tectonic movement. One of the most significant tectogeneses was the breakup of Gondwanaland during the late Jurassic to the Cretaceous which both created dextral shearing of the South African

margin bounded by the Agulhas-Falkland fracture zone and caused regional fragmentation and distortion of previous structural frames because the compressive stresses were replaced by tensile ones. However, intraplate movements were more likely to take place along the existing thrust planes of relative weakness, which led to the development of half-grabens such as the Oudtshoorn and Worcester basins where the Mesozoic strata were developed. This tectogenesis has turned most of the previous thrust faults into normal faults with a gross throw of over 6 000 m at the Worcester fault, for instance, and an impressive throw at the Kango-Baviaanskloof fault. Moreover, many of the discontinuities have been reactivated since the post-Karoo tectogenesis which complicated the existing fault systems.

Since it has been reported that in this country more than 90% of aquifers comprise fractured rocks besides fracture networks, the structural voids associated with faults constitute important spaces allowing groundwater to be stored and to move. Regardless of the fault type, a fault zone may act as a localized conduit or barrier to groundwater, depending on the properties of the fault architecture represented by the fabrics of the fault core and damage zones on both sides of the fault. As mentioned above, the type and properties of a fault could likely be changed over times due to different

patterns of crustal driving force occurring in different tectonic stages. In this regard, a normal fault developed in hard rock terrain is more likely to be a preferred locality for groundwater exploration and exploitation, attributed to the tensile stress acting on the fault, resulting in more open fractures developed along the fault zone.

It is not necessary, however, to hold the perception that groundwater occurs on a fault zone that is attributed to dense fractures and high porosity of core materials along the fault. Unlike in many other countries where the fault core materials of the Quaternary active faults are mostly uncemented, neotectonic activity in South Africa characterized by a lack of recent terrace and planation surfaces is of low magnitude. As a result, very few faults have been affected by recent neotectonic movement. In fact, most of the fault zones developed in hard rock terrains have been evidenced to be lithified and to act as aquicludes, in spite of the existence of localized zones with tensile stress concentrations or faults developed in karstified rocks with dual porosity. However, the weathering depth along a fault zone is usually larger than that of the country rocks. The weathering process is one of the key factors that impacts on the current occurrence and distribution of groundwater in fractured rocks.

Therefore, similar to all the other scientific researches, this study is also started with the classification of faults, and the classification is basically on a basis of fault zone permeability, porosity and connectivity of pore spaces or fractures. Owing to the particularity of the fault architecture and spatial extension, its hydrogeological properties may change in the directions along fault strike and normal to the fault. Moreover, compared with the country rocks, fault zone material is more susceptible to the weathering process, and its hydrogeological properties may also change at depths. Therefore, the key aspects of the research associated with fault-controlled aquifers are the investigation of the development of a fault from the perspective of structural geology, conceptualization of the fault aquifer from the perspective of hydrogeology, as well as the identification of fault zone heterogeneity and associated hydraulic properties. And all these were used to contribute to the establishment of the fault aquifer conceptual model for the purpose of groundwater quantification that was conducted at the late stage of the study.

Characterization and conceptualization of fault aquifers

Based on the understanding and review of previous researches, the fault aquifers can be classified into: 1) localized conduit; 2)

distributed conduit; 3) localized barrier, and 4) composited conduit/barrier to groundwater flow and storage. This forms the basis of aquifer characterisation and conceptualization.

Similarly to dykes, a major fault and its secondary splays are important localities for groundwater targeting in South Africa, and the majority of fault zones developed in the hard rock terrains have been evidenced to be lithified and act as aquicludes. However, the current state of a fault is the combined result of geological and geomorphological processes. Geologically, neotectonic activities might have the most recent impact on fault architecture, notwithstanding the activities are reported to be low in frequency and magnitude, which may lead to the concentration of localized tensile stress. Geomorphologically, the weathering process has played a very important role in modifying fault zones from previously cemented aquicludes into localized conductive zones. Therefore, there might be a number of localized aquifers along a fault zone. During the review of the South African faults database and associated borehole information, it was difficult to determine the pattern of groundwater concentration along a fault with a scale of tens to hundreds of kilometers long. On a site scale, the most common fault aquifer media which influence groundwater occurrence include weathered fault cores and highly permeable damage zones.

In order to select a site for further research, besides a general review of fault structures, two case studies for the Taaibos fault in Alldays, Limpopo, and the Watervalkloof fault in Rawsonville, Western Cape, were conducted. According to the results from previous exploration done extensively along the fault zone in the 1980s by using geophysical surveys, borehole drilling and pumping tests at selected wells, the Taaibos fault zone is highly fractured with fault core material weathered up to a limited depth. As a result, groundwater largely occurs on the weathered fault core with boreholes drilled to a depth never in excess of 80 m.

In contrast, groundwater occurs in the damage zones of the Watervalkloof fault, with a site at Rawsonville characterized by the presence of an unconfined aquifer in the east damage zone and a confined aquifer with artesian flow in the west. In this case, aquifers can be regarded as composite groundwater conduits/barriers where fault core material is completely impervious. In fact, the understanding was gained from the results of previous multiple approaches to investigating the fault aquifer; these approaches include well drilling, the establishment of a borehole network, borehole core logs, in-situ fracture measurements and hydraulic tests. Therefore, the site was selected for conducting further research for which an additional pumping test and constant head

test were respectively conducted in borehole BH-3 and borehole BH-1. Additional results of site measurements and hydraulic tests are summarized as follows.

As highly fractured rocks that directly ride above the fault plane represent a zone of high transmissivity and potentially high storage, this helps to understand the properties of the other large scale faults and their impact on groundwater flow.

At this site, groundwater only occurs on fault damage zones. It is hence important to determine the thickness of the damage zone. This value is defined via an analogical study, particularly the studies of faults developed in sandstones.

According to previous studies, the damage zone thickness is closely related to the fault throw. The thickness is 1.6 to 2.5 times the fault throw in this case, and is estimated at around 500 m.

It was noted that no flow condition of the fault remained unchanged due to the unchanged flow rate observed at artesian borehole BH-1 in the west (with confined aquifer), while pumping tests with different flow rates were done at borehole BH-3 in the east (with unconfined aquifer) in 2006 and 2013, respectively. This suggests that the fault plays the role of barrier to groundwater in the occurrence of groundwater at this site.

Through comparative analyses with data derived from pumping tests in 2006 and 2013, respectively, it was also noted that various pumping rates at the same borehole did not substantially change the intrinsic hydraulic properties K and S values of the aquifer. However, the observed time-drawdown patterns of the two tests were different, especially at the dewatering stage of early times. This suggests that it is not appropriate to use the observed drawdown at early time for the estimation of aquifer properties.

The final drawdown of the October 2013 pumping test in the BH-3 is 24.47 m and the drawdowns in the other two monitoring holes BH-2 and BH-5 were respectively 8.88 m and 17.25 m. This result is similar to that of the constant discharge test done in November 2006, which reveals an anisotropic property of bulk transmissivity of the aquifer.

Analytical results of both recent and previous pumping tests show that unconfined aquifers at the fault damage zone can be an important source for sustainable water supply due to the stabilization of the time-drawdown curve that occurred at the late stage of both pumping tests. However, how to sustainably utilize this fractured rock aquifer cannot be determined in quantity via the analysis of pumping tests, because this method seems to be too ambitious in fractured rock aquifers and such a lesson

was learnt from a number of well fields associated with fault aquifers in South Africa, where the water level at the production borehole continued to lower after a few years of pumping at a flow rate derived from pumping test data analysis. In order to maintain the pumping rate without continuous water level drops in the long term, it is necessary to pay much attention to the determination of sustainable yield needs to be estimated by using various methods such as hydraulic tests, surplus models based on mass principles, numerical modeling, etc.

Numerical modelling for groundwater management

Groundwater numerical modelling provides an effective tool towards the evaluation and prediction of groundwater behavior and quantity for groundwater management and contamination control purposes. A three dimensional modelling was performed with a case study of the fault aquifer at the Rawsonville site. The software Feflow 6.0, based on finite element codes, was applied to simulate groundwater flow within the unconfined fractured rock aquifer which is proved to have close interaction with the stream running through the site area. With respect to the confined aquifer in the west side of the fault, except for the artesian borehole BH-1, there is no additional observation hole to assist in modelling the aquifer. The modelling of the unconfined aquifer started

with a conceptual model with an understanding obtained from the results of core logging, field measurements and hydraulic tests. This modelling process attempts to:

- 1) Simulate natural groundwater flow in the damage zone by characterizing the distribution of aquifer hydraulic heads.
- 2) Examine the effects of pumping alternatives on the change of hydraulic heads with a number of constant hydraulic heads located along the stream.
- 3) Determine possible travel times of the potential pollutant driven by the flow process by using the water levels at observation boreholes as initial condition.
- 4) For groundwater management, determine the aquifer sustainable yield through analyzing the impact of groundwater abstraction on the change of groundwater regimes.

In this study, borehole leveling data were used to define the model geometry; aquifer physical and hydraulic properties used for the model input were the combined results from packer and pumping tests. Subsequently, the natural flow system without external stress and flow conditions under different pumping scenarios were simulated, respectively.

Results for the natural flow system show that a balancing groundwater dynamics with groundwater in the fault damage zone flows from the south and discharge to the north, while the four borehole network is located on the upper zone of the discharge area; and simulated water levels were well correlated with the observed water levels at boreholes.

Simulated results with different pumping alternatives show a distinct impact of groundwater abstraction on the hydraulic head, particularly in the vicinity of the pumping hole. The continuous pumping drastically changes the original groundwater dynamics reflected by the change in flow direction and the evolution of depression cones on the damage zone. A long-term abstraction slowly increases the drawdown of the water table, and the drawdown may ultimately stabilize at a certain level. However, the degree and time duration of ultimate drawdown is basically dependent on the pumping rate. As one of the results, the relationship between the ultimate drawdown and pumping rate is presented as follows:

$$s_w = 2.2189 \cdot Q_a^{1.0653}$$

where s_w is the drawdown and Q_a the pumping rate.

The empirical equation that was derived from the site specific study can be used to

determine the aquifer sustainable yield. Moreover, it provides an option for informed decision making. Issue of how to sustainably pump a particular aquifer relies on a compromise reached between the groundwater user and water authority. Based on the understanding of the aquifer setting and a regular demand for water from the aquifer at the dry season, the maximum stabilized drawdown is recommended as not more than 20 m with an optimum drawdown of 10 to 12 m, which would not have a negative impact on the ambient hydrogeological environment. Therefore the recommended amount of the pumping rate would be 4 ℓ/s to 7 ℓ/s ; correspondingly stable drawdowns would range from 9.7 m to 17.6 m.

ACKNOWLEDGEMENTS

This research project was funded by the Water Research Commission (WRC) with the assistance from the Groundwater Group, University of the Western Cape.

The project team is grateful to the chairperson of the project steering committee, Dr Shafick Adams, for his effort and patience in managing the project. Many thanks are also given to the steering committee members:

Dr S Adams (Water Research Commission)

Dr JM Nel (University of the Western Cape & GCS Water and Environment Consultants)

Dr L Chevallier (Council for Geoscience)

Dr C Hartnady (Umvoto)

Dr D Vermeulen (University of the Free State)

for their inputs to the programme from start to finish as well as their suggestions and comments.

Many thanks are given Mr E Bertram of the Department of Water Affairs (DWA) and the DWA Limpopo Office for their contributions to the research site selection of the project.

We would also like to acknowledge the interns of the Water Geoscience Unit, CGS for their plentiful assistance in the course of data collection and field testing, as well as the postgraduate students of the Department of Earth Sciences at UWC for their assistance in the fieldwork of the project.

Special thank is given to Mrs SJ van Eck of the CGS who provided valuable and constructive comments in the course of reviewing the final report.

TABLE OF CONTENTS

EXECUTIVE SUMMARY	iii
ACKNOWLEDGEMENTS.....	ix
1 Introduction.....	1
1.1 Research background.....	1
1.2 Objectives	3
1.3 Methodology	4
2 Overview of fault structure	6
2.1 Basic concept	6
2.2 Fault structures and associated property.....	6
2.3 Impact of fault on groundwater – general overview.....	8
3 Fault aquifer characterization with A site specific study.....	9
3.1 Introduction.....	9
3.2 Site description.....	10
3.3 Previous work.....	12
3.4 Pumping test.....	12
3.4.1 <i>Pump test results</i>	<i>13</i>
3.4.2 <i>Previous pumping tests.....</i>	<i>14</i>
3.4.2.1 Observed drawdown of pumping hole	15
3.4.2.2 Observed drawdown and recovery at monitoring hole.....	16
3.4.3 <i>Hydraulic properties from the pumping tests</i>	<i>17</i>
3.5 Summary of CD pumping test	18
3.6 Constant head test	20
3.6.1 <i>Hypothesis and theoretical background.....</i>	<i>20</i>
3.6.2 <i>Constant head test and data interpretation.....</i>	<i>22</i>
3.6.2.1 Constant head test.....	22
3.6.2.2 Data interpretation	22
3.7 Water quality	24
4 Conceptual model.....	26
4.1 Classification	26
4.2 Fault architecture model.....	27
4.3 Conceptual model with case study.....	29
4.3.1 <i>The role of weathering of the fault zone – fractured porous medium.....</i>	<i>30</i>
4.3.2 <i>Composite groundwater barrier/conduit – discrete fracture model</i>	<i>31</i>
5 Numerical modelling	33
5.1 Purpose and scope	33
5.2 Model configuration and data process.....	34
5.2.1 <i>Hypothesis</i>	<i>34</i>
5.2.2 <i>Surface water/groundwater interaction</i>	<i>35</i>
5.2.3 <i>Model preparation.....</i>	<i>35</i>
5.3 Boundary condition.....	36
5.3.1 <i>Model boundary</i>	<i>36</i>
5.3.2 <i>Hydraulic head.....</i>	<i>38</i>
5.4 Model processing.....	39
5.4.1 <i>Hydraulic properties</i>	<i>39</i>
5.4.2 <i>Model processing.....</i>	<i>41</i>
5.4.3 <i>Simulation result and discussion.....</i>	<i>41</i>

5.4.3.1	<i>Natural flow</i>	41
5.4.3.2	<i>Groundwater abstraction and sustainable yield</i>	44
5.5	Summary	50
6	References	52
Appendix 1 data of step drawdown test, October 2013		56
Appendix 2 Data of constant discharge test, october 2013		59
Appendix 3 Data of constant head test at borehole BH-1, October 2013		61
Appendix 4 Data of CD pumping test, BH-3, November 2006		63

LIST OF FIGURES

Figure 1 Types of fault structures (see <http://www.see.leeds.ac.uk/structure/faults/>) 7

Figure 2 Map showing geology surrounding the Rawsonville site..... 11

Figure 3 Topographic map showing boreholes and the Watervalkloof fault..... 13

Figure 4 Water level drawdown versus time in the 1440 CD pumping test of BH-3..... 14

Figure 5 Water level drawdown versus time in the 1440 CD pumping test..... 15

Figure 6 Semi-log and log-log graphs of BH-5 during the pumping test in November 2006 .. 16

Figure 7 Step drawdown data showing drawdown versus time 17

Figure 8 Step drawdown test of BH-3 drawdown versus time of Cooper-Jacob graph..... 17

Figure 9 The final drawdown after pumping test (Lin, 2008) 20

Figure 10 Constant head test at BH-1 on 14 to 16 October 2013 23

Figure 11 Flow rate against time during the constant head test at BH-1 23

Figure 12 Semi-log plot of flow rate against time during the constant head test..... 24

Figure 13 Demonstration of groundwater and surface water composition at the Rawsonville site..... 25

Figure 14 Distribution of faults and lineaments in South Africa..... 27

Figure 15 Fault zone architecture..... 29

Figure 16 Map showing the Taaibos fault and boreholes drilled in the Alldays area 31

Figure 17 Hydrogeological conceptual model of a fault-controlled aquifer at the Rawsonville site..... 32

Figure 18 Initial model area of the Rawsonville site 34

Figure 19 Model configuration..... 36

Figure 20 Conceptual model with the distribution of hydraulic conductivity assigned to the layers..... 39

Figure 21 Hydraulic conductivity plot against depth from packer tests in BH-1 and BH-2 at the Rawsonville site (after Lin, 2008). 40

Figure 22 Modelling result with a balancing water table collectively calibrated by initial and boundary conditions in an unconfined environment 42

Figure 23 Model used to estimate the travel time driven by the flow process 43

Figure 24 Effect of abstraction on the hydraulic head in BH-3 at flow of $Q=15$ l/s 45

Figure 26 Drawn from long term well abstraction at the flow rate of 15 l/s..... 47

Figure 27 Drawdown time curve derived from a simulated pumping test with a duration of five days (1 780 hours) and a flow range of 8 l/s at BH-3 47

Figure 28 Simulated drawdown by a 10 year well abstraction at various pumping rates 49

Figure 29 Relationship between pumping rate and stable well drawdown..... 50

LIST OF TABLES

Table 1 Basic information of the boreholes at the Rawsonville site	11
Table 2 Hydraulic properties from pumping tests at the Rawsonville site	19
Table 3 Major water quality parameters of the Rawsonville site	24
Table 4 Evolution of fault zone with implication of hydrogeological classification of fault	28
Table 6 Boundary and initial condition for model simulation	38
Table 7 Layer elevation and associated hydraulic conductivity and specific storage.....	40
Table 8 The comparison of the measured water level and simulated water level.....	43

1 INTRODUCTION

1.1 Research background

Water is perhaps South Africa's most critical resource – one of low abundance and a growing need. The country is located in an arid to semi-arid region where less than 10% of the rainfall is available as surface water and groundwater resources are equally limited. There is an increasing rate of development in and an accelerated demand for clean water and sanitation. The pressure for water resources hence calls for a need of preserving available water resources by all means possible and wherever possible improving the conditions in order to maintain sustainable adequate water quantity and quality. However, the persistent problems with water shortages and contamination induced by agricultural, mining, industrial and other anthropogenic activities have had a negative impact on the growth of the economy in the country. Moreover, the utilization of surface water is reaching its upper capacity and groundwater has hence strategically become a prominent resource of the nation where more than 90% of aquifers comprise hard rocks. Before utilizing the resource, it is necessary to have a better understanding of current status of the resource and its associated problems due to internal factors which control the occurrence of groundwater and external stresses such as climate change, industrial and mining activities, etc.

In South Africa, the lithology and stratigraphy of various geological formations have been studied in detail (Johnson et al., 2006) and the results have been applied to many fields of the geosciences. However, detailed information of folding and faulting structures across the country is scarcely documented. This has caused much difficulty in the study of the hydrogeology of fractured rocks associated with faulting structures, as faults are one of the most important geological structures that control the occurrence of groundwater in hard rock terrains. Fault-controlled aquifers have been one of the most important localities for water supply especially in water scarce areas due to its unique nature amongst the geological discontinuity. For example, the Melinda and the Klein Tshipise faults are identified as regional resources in the Limpopo Province. The Groenkloof fountain in Pretoria that occurs at the Malmani/Pretoria Group shale contact is also strongly affected by a northeast striking fault. Previous studies (Petersen and Parsons, 2001) show that most of the thermal springs in South Africa are somehow related to fault structures. In the Western and Eastern Cape Provinces, there are currently 11 thermal springs from The Bathe in the west to Uitenhage in the east that are all related to the regional faults which are the Worcester and Cango-Baviaankloof faults.

There are more than ten thousand faults recorded in the Geoline Database, whereas very few of them have been investigated and documented, particularly fault properties related to the occurrence of groundwater. These faults have experienced multiple stages of tectonic movement. One of the most significant tectogeneses was the breakup of Gondwanaland during the late Jurassic to the Cretaceous which both created dextral shearing of the South African margin bounded by the Agulhas-Falkland fracture zone and caused regional fragmentation and distortion of previous structural frames because the compressive stresses were replaced by tensile ones. However, intraplate movements were more likely to take place along the existing thrust planes of relative weakness, which led to the development of half-grabens such as the Oudtshoorn and Worcester basins where the Mesozoic strata were developed (Andreoli et al., 1996). This tectogenesis has turned most of previous thrust faults into normal faults with a gross throw of over 6 000 m at the Worcester fault, for instance, and an impressive throw at the Kango-Baviaanskloof fault. Moreover, many of the discontinuities have been reactivated since the post-Karoo tectogenesis which complicated the existing fault systems (Newton et al., 2006).

Therefore, it is not necessary to hold the perception that groundwater that occurs on a fault zone is attributed to dense fractures and high porosity of core materials along the fault. Unlike in many other countries where the fault core materials of the Quaternary active faults are mostly uncemented, neotectonic activity in South Africa is characterized by a lack of recent terrace and planation surfaces of low magnitude (Andreoli et al., 1995). As a result, very few faults have been affected by recent neotectonic movement. In fact, most of the fault zones developed in hard rock terrains have been evidenced to be lithified and act as aquicludes, in spite of the existence of localized zones with tensile stress concentrations or faults developed in karstified rocks of dual porosity. However, the weathering depth along a fault zone is usually larger than that of the country rocks and the weathering process is one of the key factors that impacts on the current occurrence and distribution of groundwater along the fault zone.

In terms of fault taxonomy, faults are classified as normal, thrust and shear faults, of which the types and properties could likely be changed over geological times due to different patterns of crustal driving force (Pollard and Aydin, 1988). Hydrogeologically, there are three types of faults that impact on the occurrence and behavior of groundwater at various scales, depending on the nature of fault zone material. Faults can act as (Antonellini and Aydin 1994; Caine et al., 1996):

- Hydraulic conduits.
- Barriers to groundwater flow.

- Combined conduit-barrier systems, e.g. leakage zones relative to adjacent aquifers.

The above classification is largely based on the fault zone permeability, porosity and connectivity of pores or fractures of idealized aquifer media. In the South African context, the mechanism of the fault structures that impact on the occurrence of groundwater is not yet fully understood. Research and investigation of the characteristics and patterns of these geological structures at various scales are still hence needed for groundwater management and informed decision making processes. Regardless of the fault type, a fault zone may act as a localized conduit or barrier to groundwater, depending on the properties of fault architecture represented by the fabrics of fault core and damage zones on both sides of the fault. Owing to the particularity of the fault architecture and spatial extension, its hydrogeological properties may change in the directions of strike and normal to the fault, of which groundwater dynamics might not be interpreted by using the traditional method for depression of cone when the aquifer is pumped. Therefore, the key aspect regarding the research of fault-controlled aquifers is the investigation of its evolution from the perspective of structural geology, classification of faults from the perspective of hydrogeology, as well as the identification of fault zone heterogeneity and associated hydraulic properties, and all these may contribute to the establishment of the fault aquifer conceptual model for the purpose of groundwater quantification.

1.2 Objectives

The research project aims to delineate and characterize fault-controlled aquifers in fractured rocks by using multiple approaches, to develop a sound method for the establishment of a conceptual model and to estimate aquifer properties and groundwater flow, based on established conceptual models and using well calibrated numerical models.

The main objective is to develop the conceptual models and ultimately to assess the impact of fault structures on groundwater occurrence in highly anisotropic aquifers. The main focus is therefore the following:

- Collection and documentation of all relevant hydrogeological data.
- Classification of faults based on a hydrogeological perspective.
- Determination of boundary conditions with the involvement of fault structures at various scales.
- Characterization of fault aquifers using structural geology methods and geophysical, geochemical and groundwater hydraulics approaches.
- Establishment of conceptual models for fault-controlled type aquifers as the basis of impact evaluation and flow dynamics.

- Quantitative evaluation of groundwater concentration and flow dynamics, and thus sort out the impact degree of fault structures on the occurrence of groundwater in fractured rocks.

This research adopts an approach of a comprehensive desktop review combined with field measurements and testing with six research tasks completed:

- A comprehensive literature review.
- Site selection and data gathering.
- Field measurements and tests.
- Characterization of aquifer media and conceptual model.
- Model calibration and simulation.
- Documentation.

1.3 Methodology

To achieve the abovementioned objectives, research of the project will be conducted in different phases with different activities as follows:

Phase 1 – Site selection and data collection. Relevant desktop literature review was done at the project preparation and site selection stages. Besides, to select proper sites for further studies, remote sensing imagery for most of the fault-controlled well fields and airborne EM imagery for part of the sites were used, from which valuable data directly inferred might be limited. However, this process was helpful in narrowing down the available sites, resulting in a number of site visits directly relevant to the Melinda and Taaibos faults in Limpopo Province.

Phase 2 – Field test and measurement. The site at Rawsonville with a five borehole network was selected as a case study for the fault controlled aquifer, where a 24 hour pumping test was conducted at a non-artesian hole and a constant head test was done in the artesian borehole, from which hydraulic properties of both aquifers could be estimated, respectively. In combination with previous hydraulic testing data, it became possible for the aquifer to be characterized and conceptualized. Hydraulic properties estimated from these hydraulic tests will be used for groundwater quantification at the next stage. Moreover, groundwater samples of the site were taken for geochemical and isotope analyses.

Phase 3 – Conceptualization and numerical modelling. The research of this phase focuses on the aquifer conceptualization with data derived from various sources and different scales, which leads to the establishment of an aquifer conceptual model on a statistical sense. Furthermore, a site specific conceptualization was completed based on the data from field

measurements and the results from data interpretation. On this basis, a 3-D numerical model using the software Feflow was conducted with the intention of better understanding the fractured aquifer, groundwater utilization and management.

2 OVERVIEW OF FAULT STRUCTURE

2.1 Basic concept

The nature and distribution of aquifers and aquitards in a geological system are controlled by the lithology, stratigraphy and structure of the geological deposits and formations. The structural features such as cleavages, fractures, folds and faults are the geometrical and physical properties of the geology systems produced by deformation after deposition or crystallization.

In terrains that have been deformed by folding and faulting, it is often difficult to distinguish the aquifers affected by these geological structures because of the geological complexity. In these cases the main ingredient in groundwater investigation is often the large scale structural analysis of geological setting by using existing geological information and remotely sensed imagery. With this analysis the boundary of an aquifer can be defined. For a small scale investigation, remote sensing and geophysical and borehole drilling methods are often used to explore the fault-controlled aquifer. A fault is a structural feature that may expose on a rock slope or may be buried by overlying stratum or soil layers. Hydrologically, faults can play many roles in conditioning flow. Faults that are neotectonically active and have developed thick zones of sheared and fragmented rocks with little fault gouge may be highly permeable, while those that possess a thin layer of gouge may be almost impermeable.

2.2 Fault structures and associated property

A fault is a crack across the rock formations which have been offset. Faults range in size from micrometers to thousands of kilometers in length and tens of kilometers in depth. They were formed on specific tectonic regions and provided the records of the nature of crustal deformation, which can be reflected by fault zone fabrics such as the type of fault rock, lineations and foliations in ductile or brittle shear zones. In addition to variation in size and orientation, different faults can accommodate different styles of rock deformation, such as compression and extension. For example,

- 1) Normal faulting is indicative of a region that is stretching, and on the continents, normal faulting usually occurs in regions with relatively high elevation such as plateaus.
- 2) Thrust faulting reflects compressive forces squeezing a region and they are common in uplifting mountain ranges. The largest earthquakes are generally low-angle (shallow dipping) thrust faults associated with subduction plate boundaries.

- 3) Strike-slip faulting indicates neither extension nor compression, but identifies regions where rocks are sliding past each other.

In Earth, faults take on a range of orientations from vertical to horizontal. Dip is the angle that describes the steepness of the fault surface. The dip of a horizontal fault is zero (usually specified in degrees: 0°), and the dip of a vertical fault is 90° . The material resting on the fault is called the hanging wall, the material beneath the fault is called the foot wall. The relative movement of hanging/foot walls determines the geometrical classification of faulting. There is differentiation between "dip-slip" and "strike-slip" hanging wall movements of faults structures.

Dip-slip movement occurs when the hanging wall moves predominantly up or down relative to the footwall. If the motion is down, the fault is called a normal fault; if the movement is up, the fault is called a reverse fault. Downward movement is "normal" because we normally would expect the hanging wall to slide downwards along the footwall because of the pull of gravity. Moving the hanging wall up an inclined fault requires work to overcome friction on the fault and the downward pull of gravity

When the hanging wall moves horizontally, it is a strike-slip earthquake. If the hanging wall moves to the left, the earthquake is called right-lateral (dextral); if it moves to the right, it is called a left-lateral fault (sinistral). The way to keep these terms straight is to imagine that you are standing on one side of the fault and an earthquake occurs. If objects on the other side of the fault move to your left, it's a left-lateral fault, if they move to your right; it's a right-lateral fault.

When the hanging wall motion is neither dominantly vertical nor horizontal, the motion is called oblique-slip. Although oblique faulting is not unusual, it is less common than normal, reverse and strike-slip faulting.

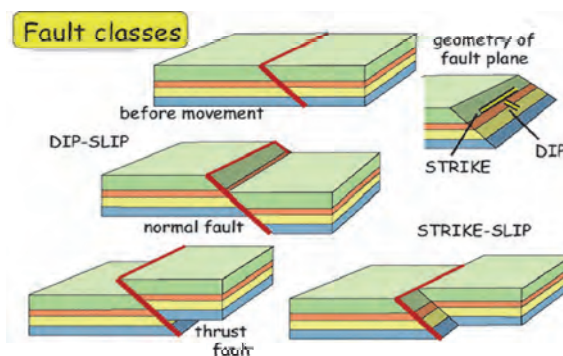


Figure 1 Types of fault structures (see <http://www.see.leeds.ac.uk/structure/faults/>)

2.3 Impact of fault on groundwater – general overview

Geological structures, such as faults, have the potential to influence groundwater flow in two contrasting ways:

- Geological material in the vicinity of a fault plane may develop fractures and openings that provide additional pathways for groundwater movement along the fault zones.
- Faults may also serve as hydraulic barriers where mineralisation and precipitation over time effectively seal the fractures created by faulting and thus limit significant movement of groundwater across the structures. Similarly, it is also possible for faults to locally displace or disconnect aquifers and obstruct lateral groundwater flow (Elhag and Elzien, 2013).

Geological structures playing different roles in groundwater quantity and quality variations include the following: groundwater reservoirs occurring in igneous, sedimentary and metamorphic rocks; voids between minerals and grains, and joints, fractures and faults (McGrath, 1994; Aydin, 2000). The distribution and composition of rocks affect the availability and chemical constituents of groundwater.

Structures as hydrodynamic contacts impact on the groundwater flow pattern of an aquifer. The major structural features impacting on groundwater are fractures and folds. Fractures are subdivided into joints, fissures and faults, which are formed by the brittle fracturing of rocks. Faults have an important role in the distribution of fluids, hydrocarbons and groundwater in sedimentary basins. Recent studies show the impact of faults on groundwater flow patterns at shallow depth (<500 m) (Bensen and Van Balen, 2004). The hydraulic behavior of faults cutting through unconsolidated sediments at shallow depth is likely to be different from that of faults at depths where rocks are lithified (>1 000 m) as fault permeability is a function of burial depth and the rheological properties of the faulted rock. Regional scale tectonic features, such as faults, shear zones and displaced blocks of the crust, exert considerable influence on the pattern and rates of interbasin and intrabasin groundwater flow (Young, 1992).

The different structures influence on and control flow by acting as low permeability zones (barriers) or high permeability zones (conduits). For example, the fault is open or closed with the logic being that if the fault acts as a conduit it will direct flow in the path of the fault, and if it is closed or weakly permeable the flow will be along or parallel to the side of the fault. In general, an open fracture will increase permeability.

3 FAULT AQUIFER CHARACTERIZATION WITH A SITE SPECIFIC STUDY

3.1 Introduction

A fractured rock aquifer is composed of a network of fractures that cut through a rock matrix. In general, fractures are referred to as geological discontinuities such as faults, joints and geological unconformities. The characterization of a fault related fractured rock aquifer requires information on the nature of both the fault and its country rock matrixes. Faults may be characterized in terms of the dimensions (fault zone extension, length, width), locations (orientation, density, etc.) and nature of the fault zone (fault core material; cementation of the core material, width and fracturing of damage zones). The rock matrix is characterized by its pore sizes and spatial distributions, often expressed by effective porosity. Generally, the hydraulic conductivity of fault zones is hundred times that of matrixes, which has been expatiated in many academic documents (Maclear, 2001; Viruete et al., 2003; Ahmadov et al., 2008; Coronado and Ramírez-Sabag, 2008). In the Table Mountain Group sandstones, for instance, the fracture systems mainly control the permeability of rock masses and are major potential pathways for fluid flow (Lin, 2008). Because the distributions and associated attributes are not uniform on either a macroscale or microscale, the anisotropy of a rock aquifer makes the determination of aquifer properties and groundwater flow paths difficult.

Ideally, to study a fault-related aquifer, the aquifer properties of the country rocks should be first investigated as a background. For the fault damage zone, aquifer media data should be gathered on the lithology, fracture length, orientation, aperture and density for developing a statistic or determinative model. Particularly the interconnection of fractures may play a key role in the determination of the groundwater flow path. It is at times difficult to have all the data for the characterization of fractures at a regional or site scale. In this sense, some level of useful knowledge can be inferred based on the structural analyses of an area or a site. The tectonic and depositional history of a given area is generally available in the geological literature (McCathy and Rubidge, 2005; Newton et al., 2006), which provides a concrete background for understanding the formation of fault-related fractured rock aquifers. For the characterization of fault core, the fault core material needs to be carefully examined via drilling or an exploration pit to ensure that the lithology of the fault core is appropriately identified. Because the fault cores are often susceptible to weathering, compared to country rocks, the determination of the depth of a weathered zone becomes one of the first priorities in studying the fault aquifer. It is of importance to determine the location of a highly conductive zone in the aquifer.

Hydraulic conductivity and aquifer transmissivity and storativity are frequently used as the key parameters to represent aquifer properties and to determine the aquifer's abstraction potential and sustainable yield. However, uncertainty and diversity of testing results often arise from various testing methods at the same site or from multiple interpretation methods using the same testing data. To estimate the hydraulic properties associated with groundwater flow and storage, multidisciplinary approaches, such as geophysical and geochemical methods, in-situ hydraulic and laboratory tests, and digital processes and numerical models (Karasaki et al., 2000; Kulatilake et al., 2003; Zhang et al., 2002, Serzu et al., 2004), are often employed. However, it is necessary to collate and analyse the data derived from different approaches, based on the understanding of aquifer hydrogeological settings. Therefore, investigation and characterization of the aquifer are crucial to study the aquifer setting, which presents both geometrical and hydraulic features of the aquifer media involved. Moreover, the development of a conceptual model for groundwater quantification is heavily dependent on the aquifer characterization and the analysis of hydraulic properties.

According to the objectives of the study, this study would place a focus on the fault aquifer characterization via the interpretation of data derived from the field test and site measurement to characterize the fault controlled aquifer at the site near Rawsonville, Western Cape. The site tested includes recent pumping tests conducted in the BH-3 and a constant head test in BH-1. Besides, groundwater quality and isotope analyses of the water samples are also presented in this study.

3.2 Site description

In 2006, a site established for groundwater research and monitoring in the fractured rocks of the Table Mountain Group (TMG) consists of a well field of five boreholes on the Gevonden farm, which is located 6 km west of Rawsonville, Western Cape. On the site, the outcrop area consists of the Peninsula, Cedarberg and Pakhuis Formations of the TMG, with minor Nardouw Subgroup, which forms a confined aquifer condition (Fig. 2). The Watervalkloof fault northeastwards extends some 15 km cutting through the well field. Controlled by both fault structures and the NE-trending TMG terrains, geomorphological features of the area are mainly characterized by the steep bared rock slopes on the Peninsula outcrop, the stepwise stream course on which there are three waterfalls with altitudinal drops of 14 m to 40 m, and a 6 m thick pluvial boulder soil covering the lowest part of the site. Several springs on the upper stream are identified but are not linked to one another in a regional flow system because the water head gradient may reach more than 1/20 just by a rough estimation on the 1/50 000 topography map.

On this site, boreholes BH-1 and BH-2 are coring holes, boreholes BH-4 and BH-5 are percussion holes, and borehole BH-5 is an existing percussion hole. The basic information of the site is listed in Table 1 (Lin, 2008).

Table 1 Basic information of the boreholes at the Rawsonville site

Borehole No.	Coordinate (°)		Type	Depth (m)		Current water level (m amsl)	Collar Elevation (m amsl)
	E	S		Bore	Casing		
BH-1	19.24615	33.71846	Ø75mm, core drilling, incline	250	156	287.30	286.825
BH-2	19.24659	33.71853	Ø75mm, core drilling	201.1	65	285.92	285.924
BH-3	19.24696	33.71790	Percussion	200	16	282.24	283.341
BH-4	19.24654	33.71809	Percussion	8	6		284.634
BH-5	19.24755	33.71749	Percussion	175		283.18	284.983

A more detailed site description can be found in Lin (2008), where information with borehole core logging, initial groundwater observations, hydraulic tests and the examination of fracture characteristics for the site specific study on the aquifer's hydraulic properties are documented.

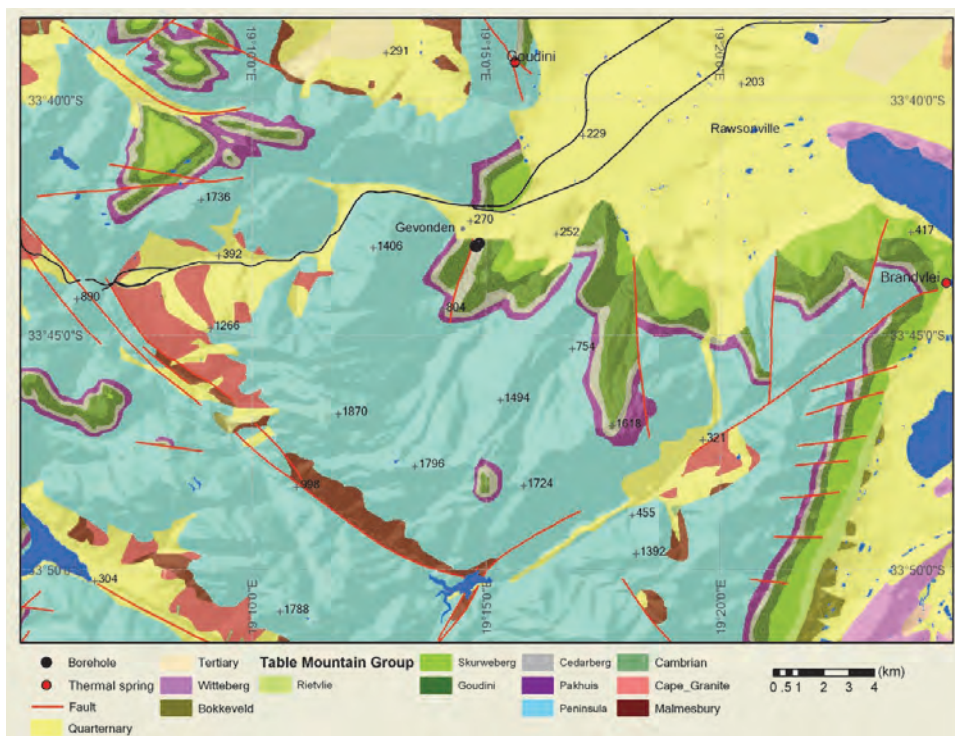


Figure 2 Map showing geology surrounding the Rawsonville site

3.3 Previous work

There are a number of research activities done for groundwater and surface water studies in regard to the site.

- In 2005-2006, the site was established via borehole installations, core logging and field measurements.
- In the same period, packer tests with an interval of 6 m were conducted, along with core drilling at boreholes BH-1 and BH-2.
- Pumping tests with a flow rate of 2 ℓ /s were done respectively in boreholes BH-3 and BH-5.
- Surface ^{222}Rn surveys to indicate the concentration of groundwater were done in the site area.
- After the above activities, some additional groundwater studies such as groundwater protection zoning (Nel, 2011; Dustay and Nel, 2013) and the identification of fracture flow (Nel, 2011) were also conducted at this site.

3.4 Pumping test

A pumping test is a practical, reliable method of estimating well performance, borehole yield, the zone of influence (drawdown) of the borehole and aquifer characteristics (i.e. the aquifer's ability to store and transmit water, aquifer extent, presence of boundary conditions and possible hydraulic connections to surface water bodies). The pumping test, sometimes also called aquifer test, may consist of pumping groundwater from a borehole usually at a constant rate, and measuring water levels in the pumped borehole and observation boreholes nearby.

An aquifer test with the duration of 48 hours was conducted to evaluate the hydraulic or aquifer parameters in the Watervalkloof fault zone on the Rawnsenville site. Borehole BH-3 was used as the pumping borehole during the aquifer test conducted in late October, 2013. On the site, only borehole BH-3 and borehole BH-5 are deep percussion holes and BH-3 with a depth of 200 m seems to have the highest yield and is completed only in the deep aquifer. Dip meters were installed in each borehole to monitor water levels prior to, during and after the test. The pump installed in BH-3 was placed at a depth of 50 m below surface and was below the open fracture zone. The pumping rate was 6 ℓ /s during the abstraction period. After the pump was shut off, the recovery was monitored in BH-2 (51 m) and BH-5 (44 m) until the water levels asymptotically reached new equilibrium values.

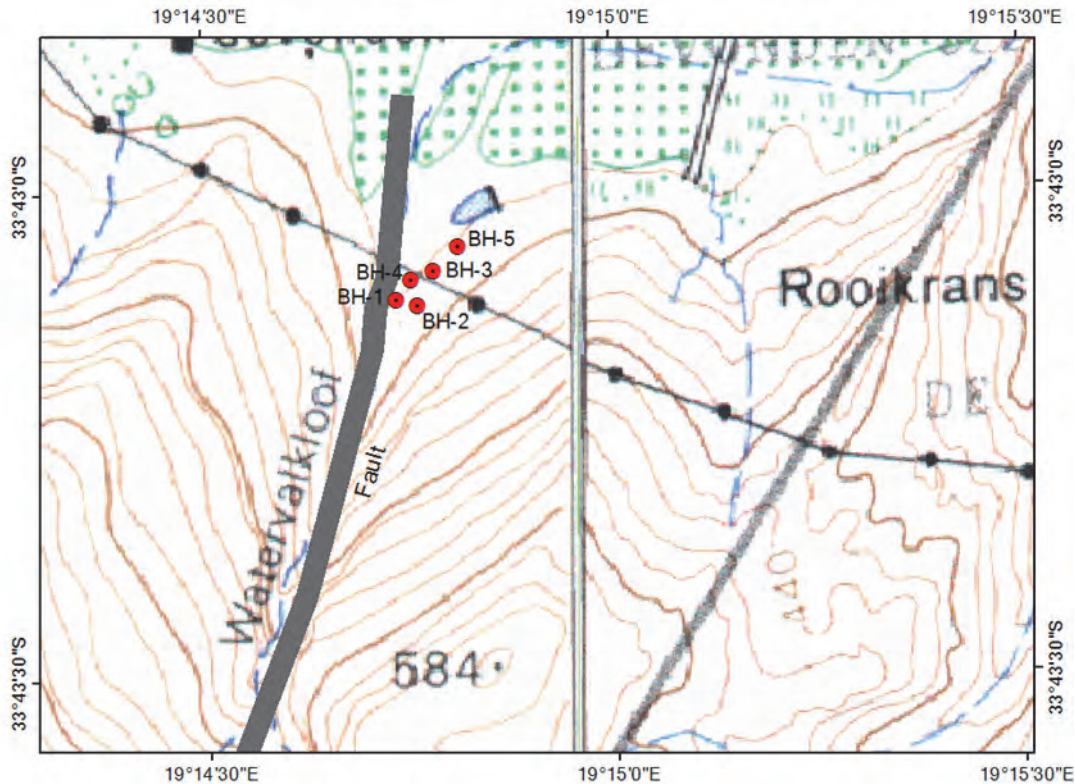


Figure 3 Topographic map showing boreholes and the Watervalkloof fault

3.4.1 Pump test results

Time drawdown plots were constructed for boreholes tested on the Rawnsenville site (see Fig. 4). In this figure, slope A shows a slope of 1 and is a wellbore storage which may come from sideways of the fracture zone. This is an early time of the water level drawdown that occurs after effects of borehole storage and skin effect have ceased to dominate the response. The T-value at this stage is represents the early time response to pumping indicates that the time drawdown plot has a unit linear slope on the log-log graph. This response may indicate an extremely transmissive fracture network or a transmissive fracture set with significant wellbore storage effects (Kruseman and De Ridder, 2000).

The second slope, B, shows a flattened curve that typically lies below that predicted by the Theis curve of non-radial flow, implying water may come from all directions due to the fault matrix of the area. This is attributed to the fact that BH-3 was drilled in a fault zone.

Finally, Slope C was recorded over a late time period. As the slope curve exceeds that of the early time period, the T-value is more representative of the effective transmissivity of the rock mass surrounding the pump borehole. The drawdown curve provides an estimate of the bulk transmissivity of the microfractured rock matrix (Fig. 4). Late time response corresponds

to a period of pseudo radial flow, which may indicate contributing flow from lower permeability fractures that intersect the fault zone.

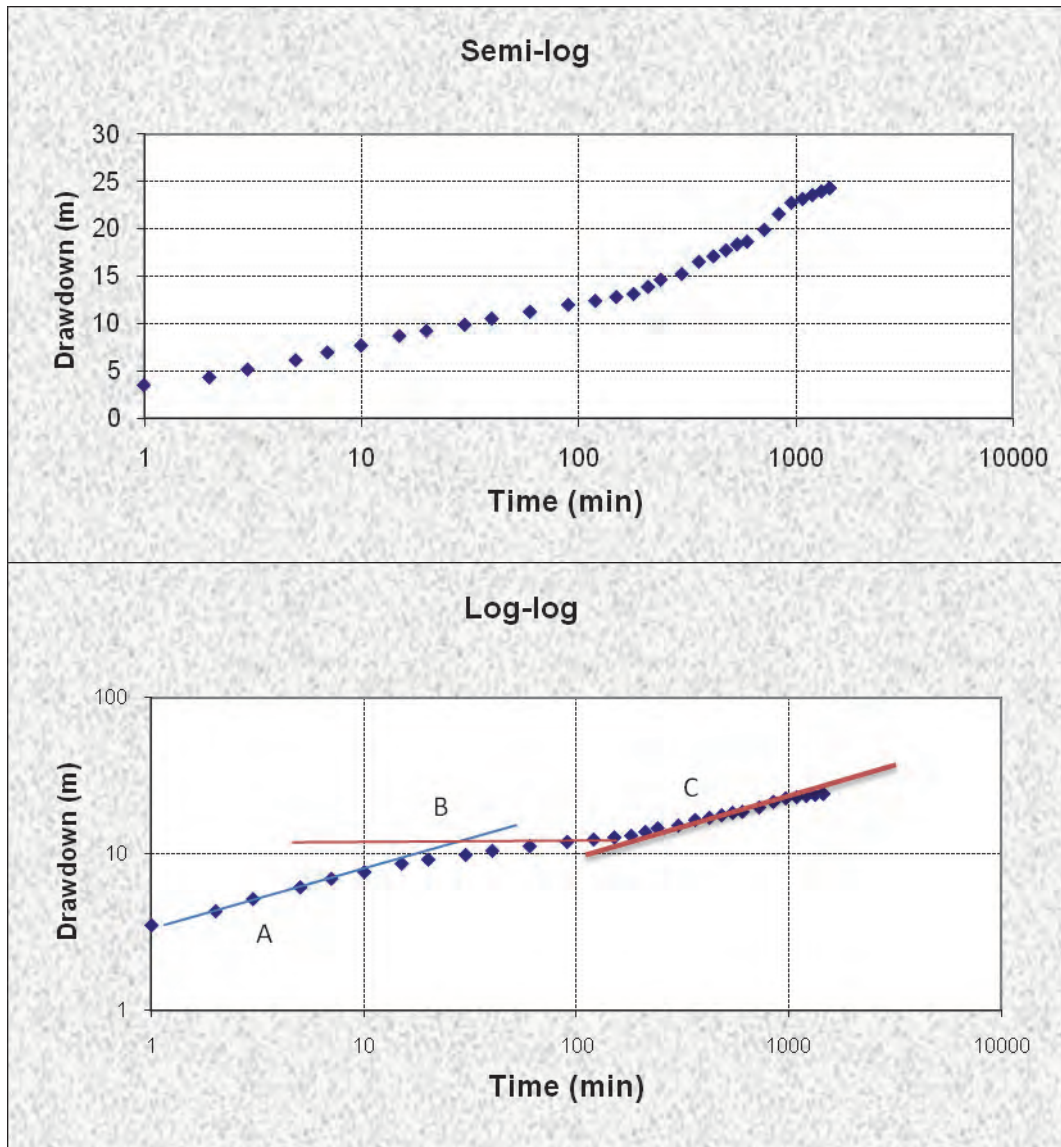


Figure 4 Water level drawdown versus time in the 1440 CD pumping test of BH-3 showing three distinct phases of flow

3.4.2 Previous pumping tests

In November 2006 the same borehole was tested for aquifer parameters at a flow rate of 1.8 ℓ/s with constant discharge, though step-drawdown was not performed then. BH-3 was drilled along fault zones in the research site.

3.4.2.1 Observed drawdown of pumping hole

The log-log plot and semi-log plot of Figure 5 collectively present the responses for the borehole that pumps vertical fracture in the unconfined aquifer of low permeability as the flow rate was set at 1.8 liters per second. Due to the lower flow rate, it was noted that the phase of the early dewatering stage was not obvious, compared with that of October 2013. The fracture would have finite length and high hydraulic conductivity. Characteristics of the system are that a log-log plot of early pumping time shows a straight line of slope 0.5.

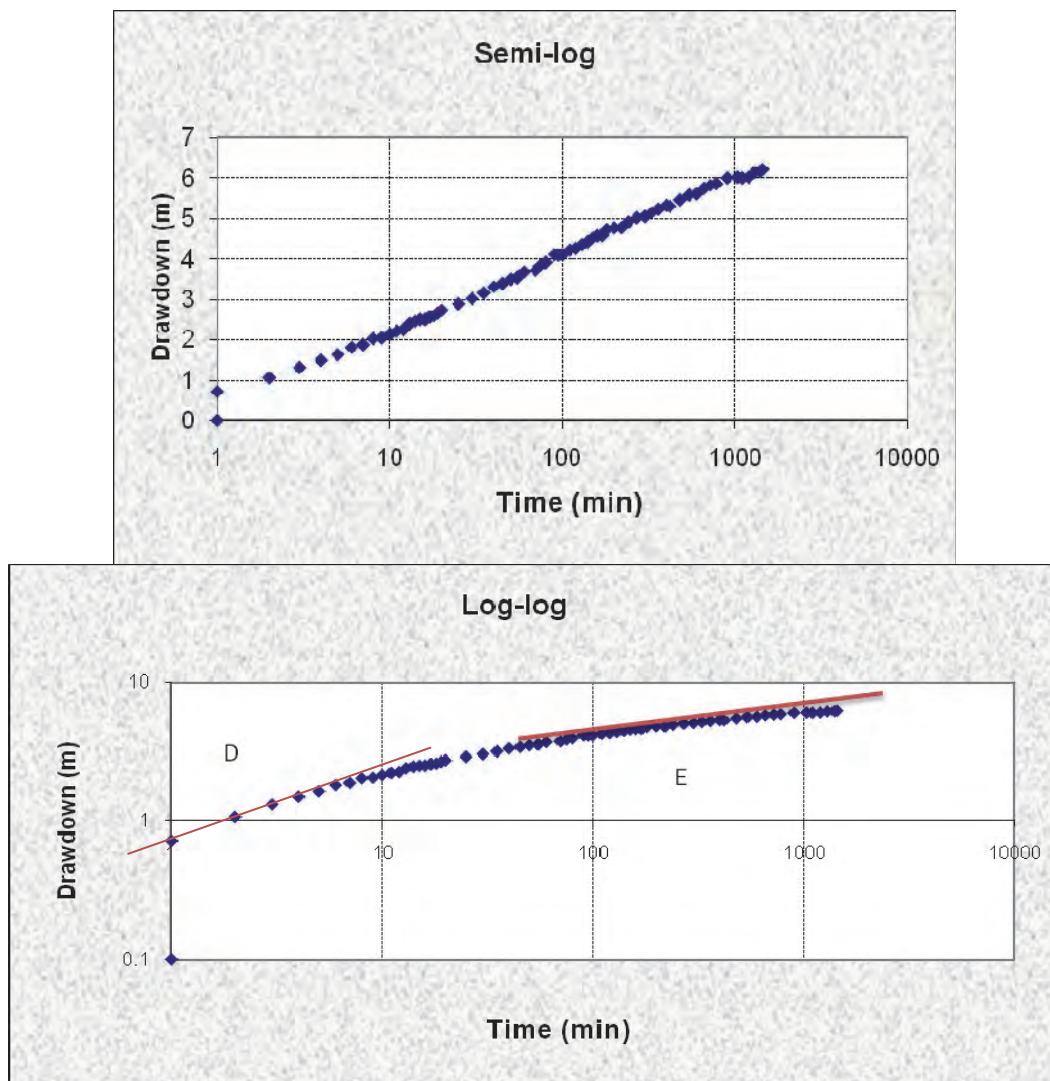


Figure 5 Water level drawdown versus time in the 1440 CD pumping test of BH-3 in November 2006

The log-log plot of Figure 5 reflects the dominant flow regime that is horizontal, parallel and perpendicular to the fracture. This flow regime gradually changes at late time (E) and becomes pseudo radial flow (after 100 minutes of pumping), a flow in the fracture which acts as an extended well.

3.4.2.2 Observed drawdown and recovery at monitoring hole

The semi-log plot shows an ideal situation where there is no influence in early pumping up to 15 minutes and after 20 minutes that the change occurred. The log-log plot shows an early recovery in observation borehole BH-5.

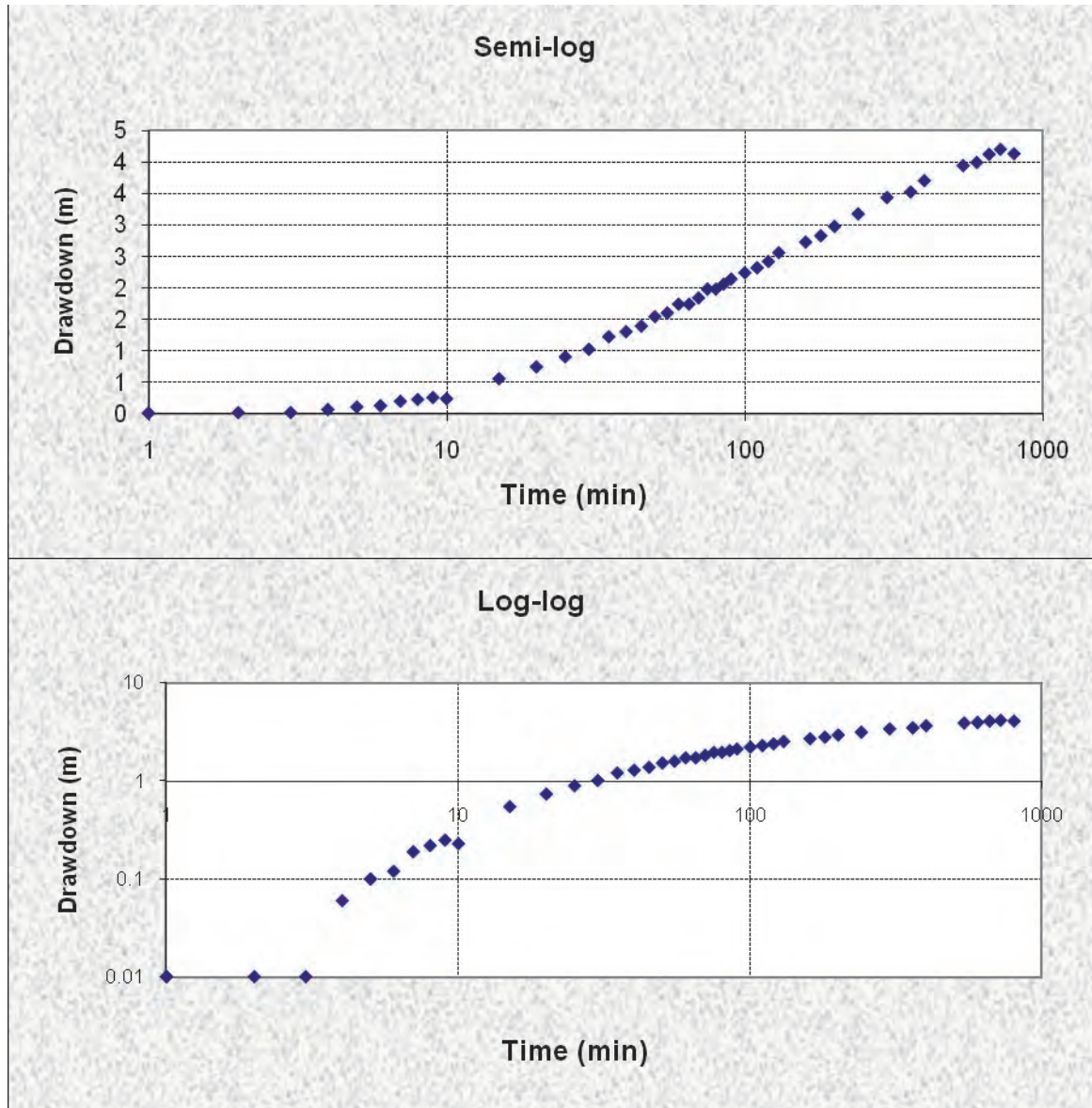


Figure 6 Semi-log and log-log graphs of BH-5 during the pumping test in November 2006

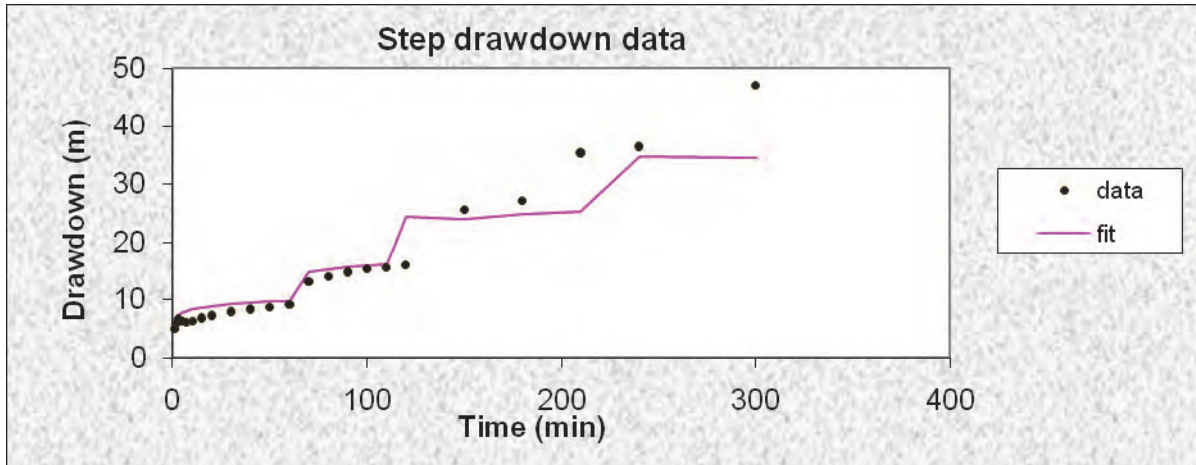


Figure 7 Step drawdown data showing drawdown versus time

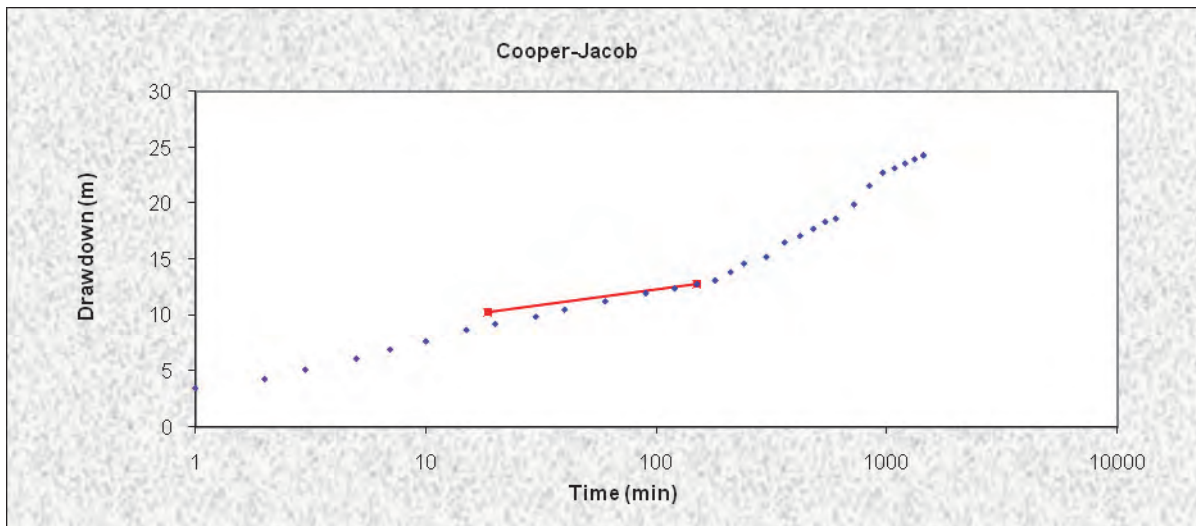


Figure 8 Step drawdown test of BH-3 drawdown versus time of Cooper-Jacob graph

3.4.3 Hydraulic properties from the pumping tests

Transmissivity was estimated using the Cooper-Jacob method for the late-time response to pumping. Drawdown data indicate that the late-time data (generally after 150 min) look more like the response of a porous media system and fall on a straight line on a semi-log graph.

The estimates of the transmissivity (T) and storage coefficient (S) using constant discharge test data of November 2006 were slightly different compared to the value of the test data of October 2013. For the later data, the T-value from the borehole BH-3 test was estimated at 12.76 m²/day or 1.48×10⁻⁴ m²/s, while the S-value was 2.17×10⁻². The T-value and S-value from observation borehole BH-5 gave estimates of 12.32 m²/day (or 1.43×10⁻⁴ m²/s) and 3.30×10⁻⁷, respectively.

The estimated transmissivity and related storage coefficient values are affected by the interconnectedness of the fracture systems between the pumping borehole and the observation boreholes. The late time estimate of T-values using the Cooper-Jacob method was 34.5 m²/day of the aquifer system. Storage coefficient (s) in an early time period was 2.20×10⁻³ and at later time period the C-J method gave an S-value of 9.27×10⁻⁸.

Using the same FC program, the results from the CD test of November 2006 are slightly different from that of October 2013, especially the S-value, where the T-value is estimated as 15.4 m²/d or 1.78×10⁻⁴ m²/s or a K value of 8.91×10⁻⁸ m/s, and the S-value is 1.99 for the late time data.

3.5 Summary of CD pumping test

Groundwater flow in the Watervalkloof fault in Rawsonville is a complex process that is controlled by the geologic variability in the subsurface. Specifically, structural variability associated with faults in the area plays an important and sometimes key role in influencing the quantity of storage and depth of flow circulation within the aquifer system.

- From the field observation of both pumping tests in 2006 and 2013, with different flow rates, it was noted that there were no flow changes happening in artesian borehole BH-1, which suggests that the fault plays a role as barrier to groundwater circulation around this site.
- Through the comparative analyses with pumping test data of 2006 and 2013, it is noted that the change of pumping rate almost does not change the intrinsic hydraulic properties of the K and S values. However, the time drawdown patterns of the two are different, especially at the dewatering stage of early time.
- The final drawdown of the October 2013 pumping test in BH-3 was 24.47 m. In the other two monitoring holes BH-2 and BH-5 were respectively 8.88 m and 17.25 m. This result is similar to that of the CD test in November 2006 (Fig. 9), which implies that the bulk T or K aquifer is anisotropic.
- These pumping test analyses reveal that fault zones can represent an important water resource for individual and municipal use, and that identification of these features is important. These fault zones may occur at greater depths as the pumped borehole (BH-3) was drilled to a depth of more than 200 m below ground surface.

- Highly fractured rocks directly above fault planes can represent zones of high transmissivity and potentially high storage. It is necessary to understand the existence of large-scale fault zones and their impact on groundwater flow.

The above estimation of T and S values is based on the Cooper-Jacob method derived from the Theis theory which assumes the aquifer as an isotropic medium. However, the pumping test data were gathered from an aquifer that is actually bounded by the fault acting as a groundwater barrier. Therefore, the image well method (Ferris et al., 1962) is introduced to estimate the hydraulic properties by positive superposition of the drawdown of the image well at the pumping hole, which is expressed as:

$$s = \frac{Q}{4\pi T} [W(u_1) + W(u_2)] \quad (1)$$

with an increase in pumping time the well function in the pumping hole ($W(u_1)$) and image well ($W(u_2)$) both tend to be less than 0.01. Equation (1) can be presented by the Cooper-Jacob formula.

$$s = 0.366 \frac{Q}{T} \lg \frac{2.25Tt}{r_w \cdot r_m S} \quad (2)$$

in which r_w and r_m are the radius of the pumping well and the distance from the pumping well to the image well, respectively, and T is transmissivity and S aquifer storativity. The distance from BH-3 to the fault is 18 m and that of BH-5 is 30 m. It is clear that the T and K values are higher than those estimated by the radial flow method (Table 2).

Table 2 Hydraulic properties from pumping tests at the Rawsonville site

Hydraulic properties	Borehole BH-3		Borehole BH-5		
	Radial flow		Image well	Radial flow	Image well
	Withdraw	Recovery	Withdraw	Withdraw	Withdraw
T (m ² /s)	1.7×10^{-4}	8.0×10^{-5}	4.5×10^{-4}	7.1×10^{-5}	1.2×10^{-4}
K (m/s)	8.8×10^{-7}	4.0×10^{-7}	1.8×10^{-6}	4.2×10^{-7}	7.9×10^{-7}

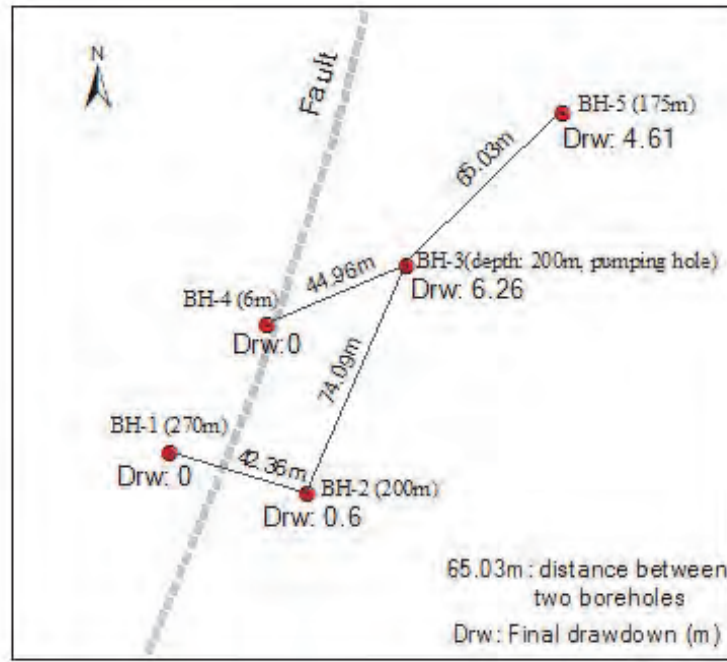


Figure 9 The final drawdown after pumping test (Lin, 2008)

3.6 Constant head test

3.6.1 Hypothesis and theoretical background

A constant head test is normally done for an artesian borehole such as borehole BH-1 at the Rawsonville site to characterize the confined aquifer and to determine the aquifer properties. The test is based on the fact that in a period of duration, the water head of the borehole does not change, while the flow rate gradually reduces to a constant value (Q). From observed data, the T and S values can be roughly estimated by using the following equations (Xue, 1986).

$$\begin{cases} \frac{1}{r} \frac{\partial}{\partial r} \left(r \frac{\partial s}{\partial r} \right) = \frac{S \partial s}{T \partial t} & t > 0, \quad 0 < r < \infty \\ s(r, 0) = 0 \\ s(\infty, t) = 0 \\ s(0, t) = s_w \end{cases} \quad (3)$$

where the assumption of equation (3) is the same as for the Theis equation. T and S are transmissivity and storage, respectively, while the s_w is the water head and r the radii of the aquifer.

Combed with Darcy's law and the derivative of the above equation may yield:

$$Q = 2\pi T s_w G(\lambda) \quad (4)$$

Where, $G(\lambda)$ is the flow function with constant head of the confined aquifer with no leakage happening in the vicinity of the aquifer; and

$$\lambda = \frac{Tt}{Sr^2} \quad (5)$$

The equations 4 and 5 can be rewritten in the form of logarithmic, which is

$$\lg Q = \lg G(\lambda) + \lg(2\pi T s_w) \quad \text{or} \quad \lg t = \lg \lambda + \lg \frac{r^2 S}{T} \quad (6)$$

This equation forms the basis of curve fitting for the estimation of the T and S values.

On the other hand, T and S can be estimated by using the linear graphical method, when

$$\lambda = \frac{Tt}{Sr^2} > 5000, \quad (7)$$

Because T and S of this aquifer are yet unknown, it is difficult to estimate the λ value of equation (7). However, from the results of previous studies, at the late time of the test, this value may meet the requirements of the equation and therefore yields the approximate expression of $G(\lambda)$, namely:

$$G(\lambda) \approx 2 / \left(\ln \frac{2.25Tt}{r_w^2 S} \right) \quad (8)$$

combined with equation (4), there is the approximate expression of flow Q

$$Q = 4\pi T s_w / \left(\ln \frac{2.25Tt}{r_w^2 S} \right) \quad (9)$$

or

$$1/Q = \frac{0.183}{T s_w} \lg \frac{2.25T}{r_w^2 S} + \frac{0.183}{T s_w} \lg t \quad (10)$$

In the case of a linear relationship between $1/Q$ and $\lg t$, there will be

$$T = \frac{0.183}{s_w i} \quad (11)$$

where i is the slope of the linear line of $1/Q$ against $\lg t$. Similarly, based on equation (10), the S value can be determined when $1/Q=0$.

3.6.2 Constant head test and data interpretation

3.6.2.1 Constant head test

The constant head test was done on 14 to 16 October 2013 (Fig. 10), with a duration of 2 650 minutes and a constant head from the ground level of 0.47 m. During the test, only the flow rate (Q) was measured at various time intervals.

- The initial flow Q was 2.22 ℓ/s when the test started and this flow only lasted not more than one minute before it substantially reduced.
- In the first 10 minutes of the test, the borehole seemed to dewater the bore storage water and accumulative hydraulic head surrounding the borehole. At the begging stage, the outflow water was a brown color and with a strong smell; the unfavorable smell did not fade away until 160 minutes into the test.
- Figure 11 shows the flow decreasing drastically in the early 250 minutes with flow Q from 2.22 ℓ/s to 0.77 ℓ/s . After that, the change of flow Q slows down and at the late time stabilizes at the level of around 0.2 ℓ/s . This is exactly the same as the flow from the third conductive zone of the borehole, reported by Lin (2008), where the first and second zones were sealed by a steel casing.

3.6.2.2 Data interpretation

The testing data is listed in Appendix 3 and plotted in Figure 11. It is noted that after 250 minutes, the flow rate at a constant head of 0.47 m stabilizes, which is assumed to meet the constraint by Equation (7). Therefore, the estimation of T and S values can be performed on the basis of Equations (10) and (11).

Figure 12 show the linear relationship between $1/Q$ and $\log t$ and their curve fitting at the late time after the time of 210 minutes. The slope of the relation i is 0.0349, and hence the bulk transmissivity $T = 1.12 \times 10^{-2} \text{ m}^2/\text{Min}$ or $T = 1.86 \times 10^{-4} \text{ m}^2/\text{s}$; the bulk hydraulic conductive of the confined aquifer is $7.44 \times 10^{-7} \text{ m/s}$. In the same way, while $1/Q=0$, the storativity S is 1.6×10^{-3} .



Figure 10 Constant head test at BH-1 on 14 to 16 October 2013

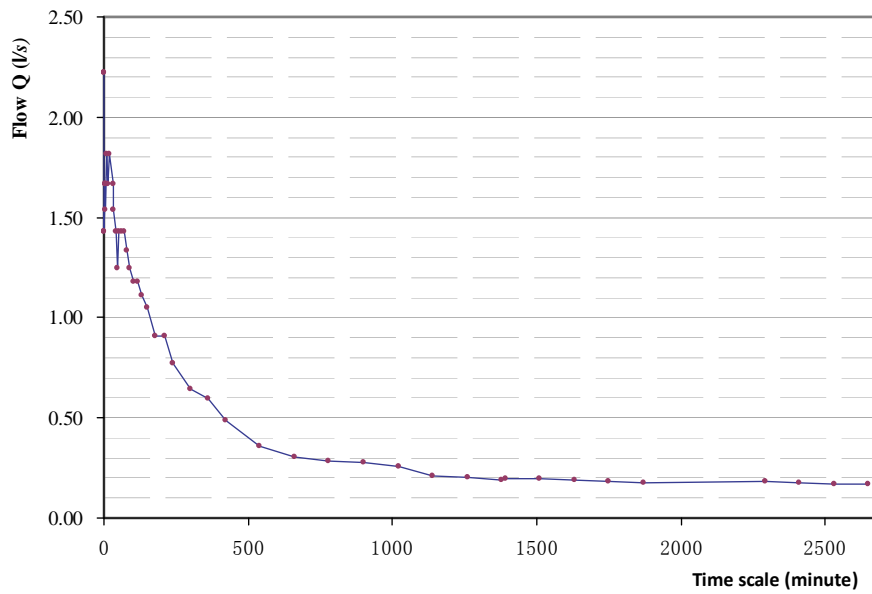


Figure 11 Flow rate against time during the constant head test at BH-1

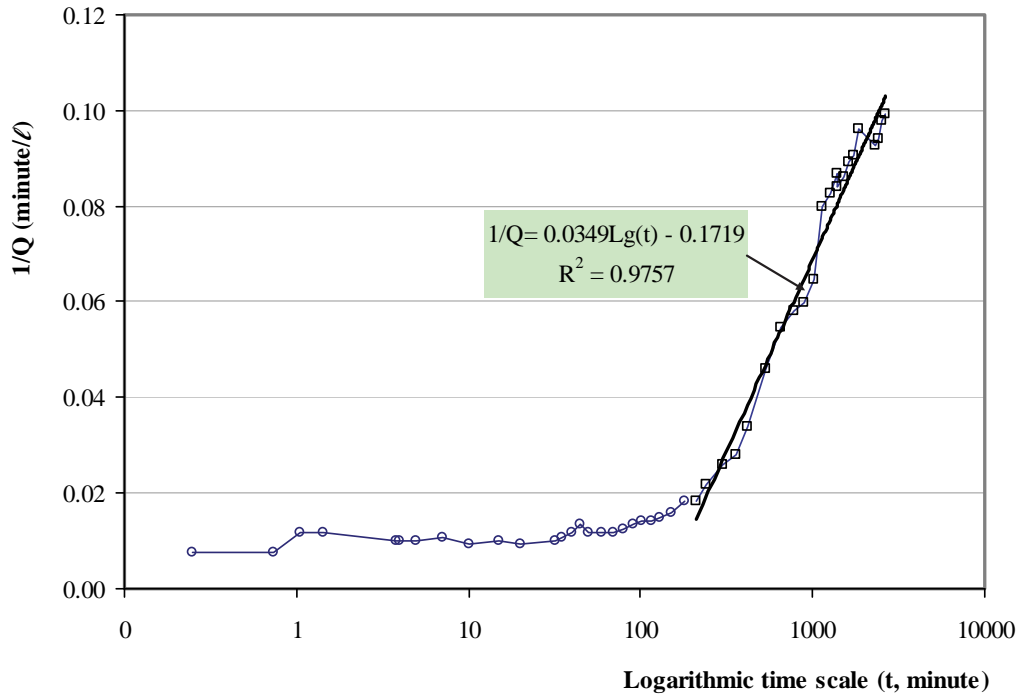


Figure 12 Semi-log plot of flow rate against time during the constant head test

3.7 Water quality

In order to examine any change in groundwater quality, the borehole and stream water were sampled three times in 2006 and once in October 2013, for which the compositions of groundwater and surface water were analysed by Bemlab and the Council for Geoscience, respectively. From the results of these sample analyses, the TDS does not change much over time which is in a range from 20 to 120 mg/kg (Table 3). However, the original groundwater type is dominated by Na-Cl type of water; but it slightly changes to be predominantly Ca-Cl water type (Fig. 13). The results show that the groundwater of this site is of good quality, except for some harmful ions such as iron (as Fe), aluminum (as Al) and manganese (as Mn) that are above limit and produce an unpreferred smell and color.

Table 3 Major water quality parameters of the Rawsonville site

Sampling site	2013			2006		
	Water type	EC	TDS	Water type	EC	TDS
		uS/cm	mg/kg		uS/cm	mg/kg
BH 1	Ca-Cl	107.4	47.27	Na-Cl	85.17	68.7
BH 2	Ca-Cl	105.7	51.4	Na-Cl	91.2	75.6
BH 3	Na-Cl	31.6	17.19	Fe-Cl	89.08	62.64
BH 4	Fe-Cl	42.31	21.45	Na-Cl	95.05	50.72
BH 5	Ca-Cl	60.61	30.53	Fe-Cl	75.52	46.71
Stream water	Na-Cl	38.36	17.52	Na-Cl	36.19	17.51

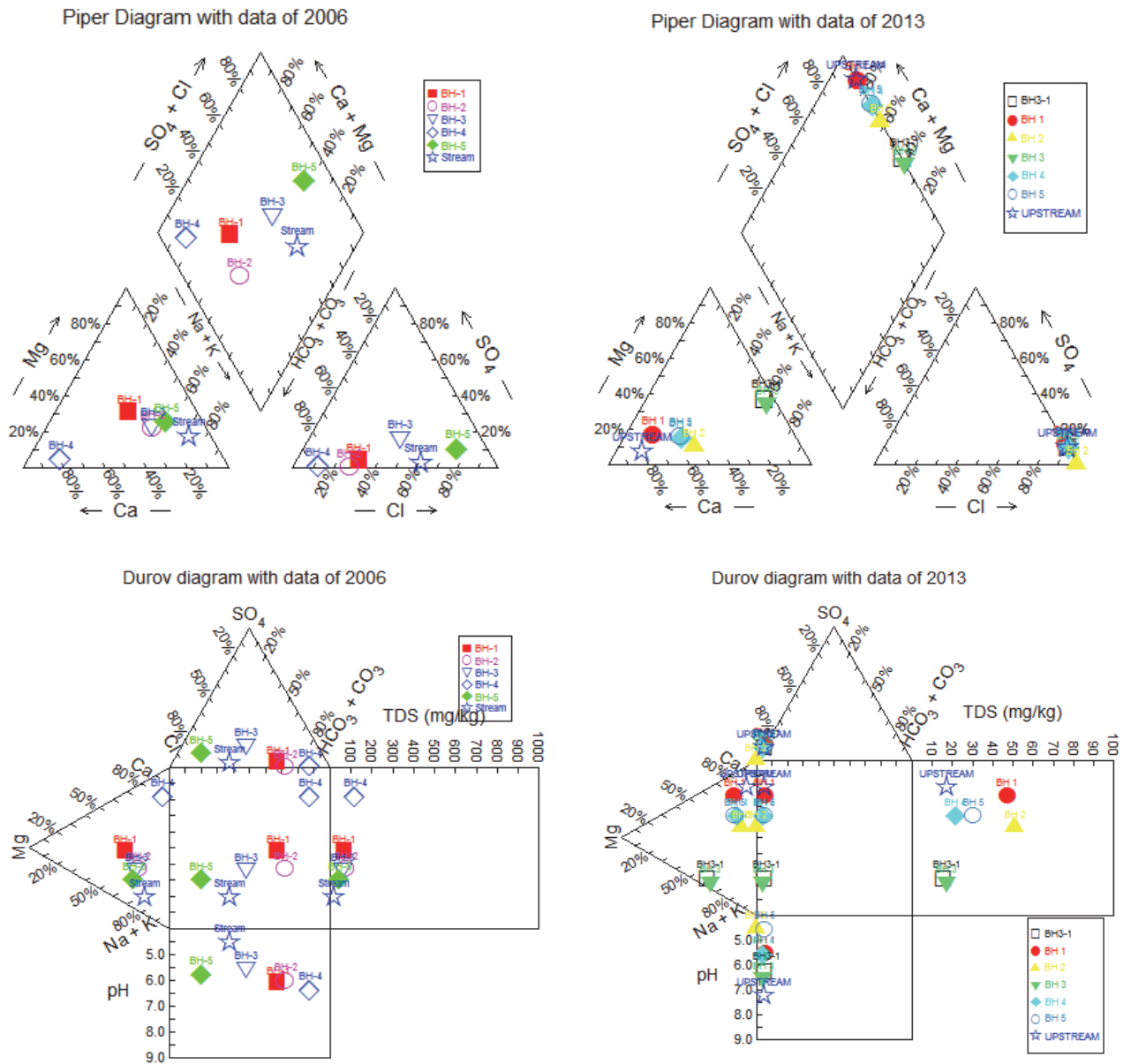


Figure 13 Demonstration of groundwater and surface water composition at the Rawsonville site

4 CONCEPTUAL MODEL

4.1 Classification

Theoretically, faults are classified into normal, thrust and shear faults, of which the type and properties could likely be changed over geological times due to different patterns of crustal driving force (Pollard and Aydin, 1988).

In South Arica, there are tens of thousands of fault records which can be primarily divided into observed and inferred faults. On a fault structure geological map, these faults are normal, thrust and shear faults, faults with unknown properties, shear zones and lineaments that are likely linear features due to faults (Fig. 14).

Hydrogeologically, there are three types of faults that impact on the occurrence and behavior of groundwater at various scales, depending on the nature of the fault zone material. Faults can act as (Antonellini and Aydin 1994; Caine et al., 1996):

- 1) Hydraulic conduits.
- 2) Barriers to groundwater flow.
- 3) Combined conduit-barrier systems, e.g. leakage zones relative to adjacent aquifers.

The above classification is largely based on the fault zone permeability, porosity and connectivity of pore spaces or fractures. Owing to the particularity of the fault architecture and spatial extension, its hydrogeological properties may change in the directions along fault strike and normal to the fault. Moreover, compared with country rocks, fault zone material is more susceptible to weathering, which suggests its hydrogeological properties may also change at depths. Hence, groundwater dynamics might not be interpreted by using the traditional method for depression of cone when the aquifer is pumped. The key aspect regarding the research of a fault-controlled aquifer is the investigation of its development from the perspective of structural geology, classification of faults from the perspective of hydrogeology, as well as the identification of fault zone heterogeneity and associated hydraulic properties; all these may contribute to the establishment of the fault aquifer conceptual model for the purpose of groundwater quantification.

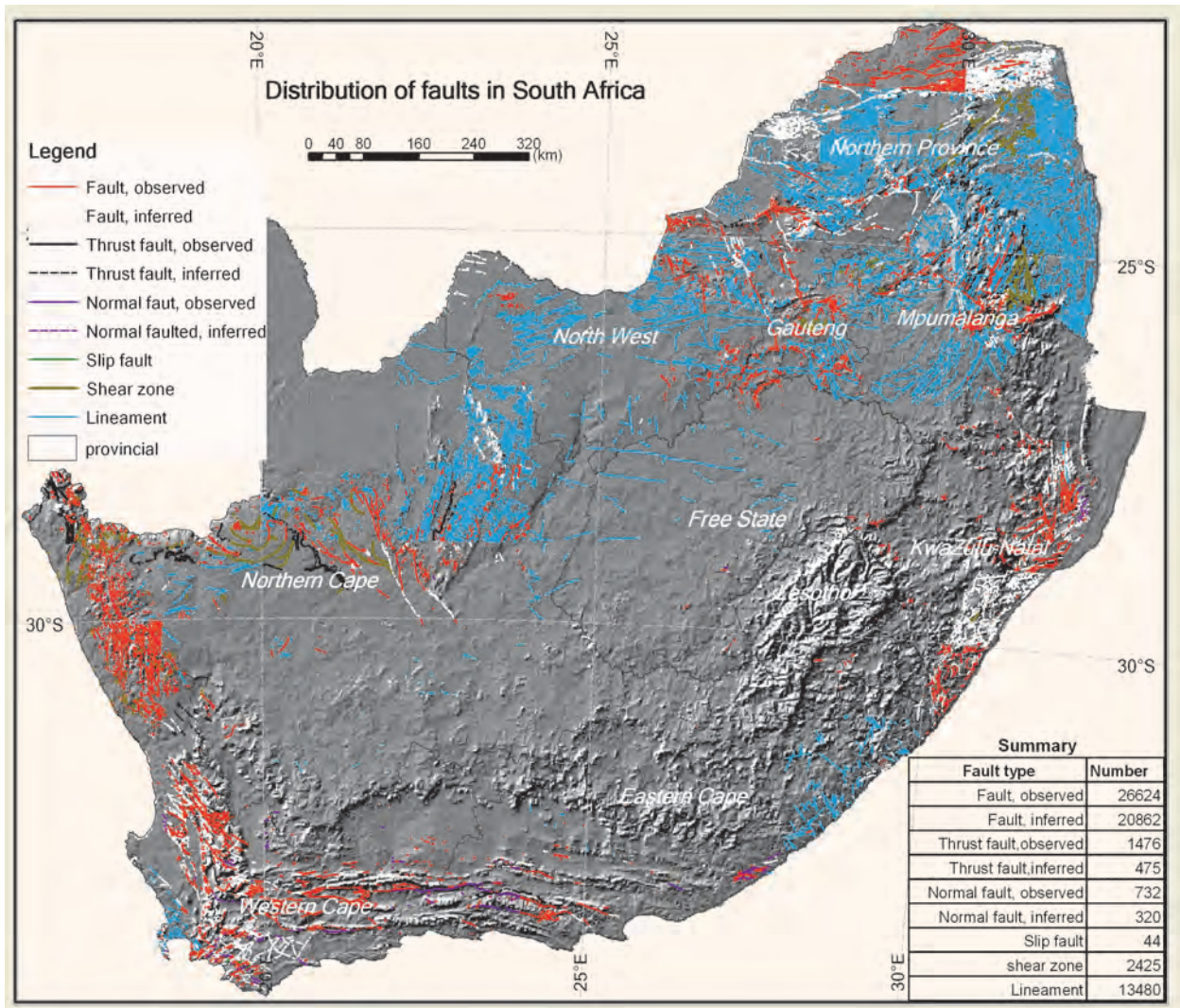


Figure 14 Distribution of faults and lineaments in South Africa

4.2 Fault architecture model

The factors that impact on the occurrence of groundwater in a fault-controlled aquifer include fault architecture. These architectural elements include fault core, fracture (damage) zones at both fault walls and country rocks (Fig. 15). The conceptual model of fault architecture was proposed by Caine et al. (1996), who used this model to delineate the development of a fault zone that is of significance to fluid flow and mineralization in the fault zone.

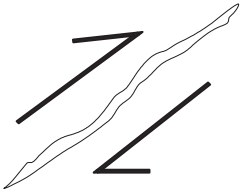

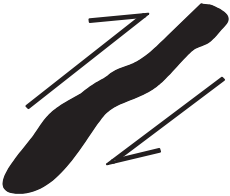

In this fault architectural model, a fault core is bounded by filled through-going slip surfaces referred to as a slip band and a surrounding damage zone which contains more joints and deformation bands compared with its adjacent country rocks. The effectiveness of a fault zone as a conduit or barrier to groundwater flow is largely dependent on the connectivity of a minor fault network and fractures within the fault damage zone and the permeability contrast between the rock matrix and deformation bands. On the one hand, the hydrogeological property of a fault core is normally characterized by geometry, composition, petrophysical

properties, porosity, permeability and the connectivity of void space (Antonellini and Aydin, 1994; Caine and Forster, 1999; Aydin, 2000; Odling et al., 2004). On the other hand, the hydrogeological property of a fault damage zone is mainly dependent on the density and connectivity of fractures and the combination of lithologies of country rock.

According to Caine et al. (1996), an evolution hydrogeological model towards the occurrence of groundwater is shown in Table 4, which in a statistical sense can be regarded as a small-scale conceptual model along with the temporal and spatial evolution of a fault. This model in Table 4 provides a classification of faults in view of hydrogeology, because it implies the significance for groundwater development, especially the development of a well field for massive water supply, if the architecture of a fault section can be identified.

Because its hydrological properties depend on the change in fault core but not the damage zone, at times problems arise from the application of this model to the actual study of fault-related aquifers; this is simply due to there being too many unknown parameters (as the above mentioned) of faults that are often required as inputs to both qualitative and quantitative models for the estimation of groundwater resources.

Table 4 Evolution of fault zone with implication of hydrogeological classification of fault

1. Localized conduit	2. Distributed conduit	3. Localized barrier	4. Composite conduit/barrier
Fault core increasing →			
			
Ideal borehole site, Large scale channel flow	Ideal borehole site Dual porosity	No flow boundary	Borehole site at fracture zones; Preferential flow; Boundary control flow and recharge

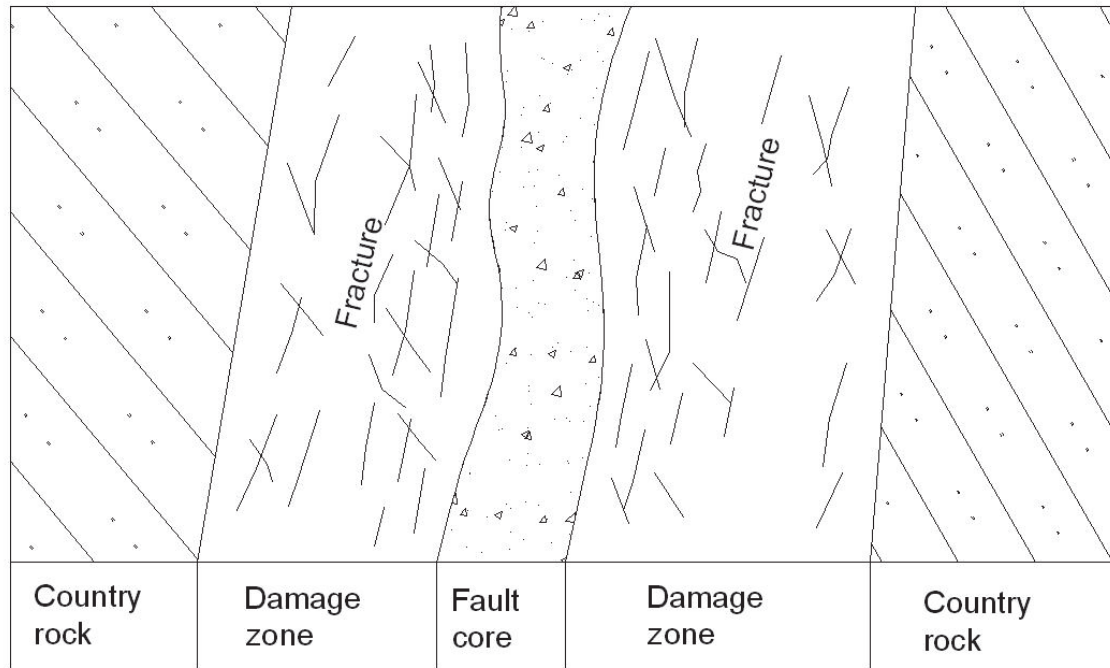


Figure 15 Fault zone architecture

4.3 Conceptual model with case study

It is well acknowledged that faults to a large extent play a key role in the occurrence of groundwater. For example, almost all the major well fields for water supply schemes in the Table Mountain Group area are developed in the vicinity of fault zones, such as Vermaak's River (Kotze, 2002), Boschklouf (Hartnady and Hay, 2002), St Francis Bay (Rosewarne, 1993a), Ceres (Rosewarne, 1993b), and so on. Where the faults intersect the regionally oriented structure they may become a preferred locality for the production boreholes.

Through field investigation in the Vermaak's River fault, Hälbich and Greef (1995) found that there were hard breccias and cataclasites widely developed in both of the 9 km long fault and its secondary splays. In the Eastern Cape, the Coega fault cutting southeastward through the Uitenhage artesian basin resulted in the separation of the basin into two different groundwater systems (Maclear, 2001). In fact, most of the fault zones developed in the hard rock terrains were evidenced to be lithified, acting as aquicludes (Newton et al., 2006), such as the Klein Bavaria fault in the north of Plettenberg Bay, the Eikenhofdam fault at Brandvlei and the Kango fault.

Similar to dykes, a major fault and its secondary splays are currently key zones for groundwater targeting in South Africa. The current state of a fault is the result of geological and geomorphological processes. Geologically, neotectonic activity might have the most

recent impact on the fault fabrics. Geomorphologically, it should be noted that the weathering process plays a very important role in modifying many fault zones from previously cemented aquicludes into localized conductive zones. Therefore, there might be a number of localized aquifers along a fault zone. In the view of South African fault information and associated borehole siting, it is difficult to determine the pattern of groundwater concentration along a fault with a scale of tens to hundreds of kilometers long. On a site scale, the most common fault aquifer media include weathered fault core or highly permeable damage zones.

4.3.1 The role of weathering of the fault zone – fractured porous medium

As above mentioned, Table 4 provides a hydrogeological classification of the fault which include the following types:

- 1) Local conduit, groundwater flow and storage is exclusively controlled by the fault core;
- 2) Distributed conduit, where groundwater is governed by both fault core and damage zones which behave as an aquifer with dual porosity or dual permeability (National Research Council, 1996);
- 3) Localized barrier, which mostly occurs in the case where a fault core is completely sealed by secondary minerals and the fault zone hosted in a country rock with very low permeability;
- 4) Composite conduit/barrier, in this case the fault core is completely sealed by secondary minerals but the groundwater controlled by the fracture network in damage zones (Lin, 2008).

It is necessary to address the fact that the above hydrogeological classification of faults can be applicable to ideal hard rock aquifers. From the perspective of aquifer medium, this classification contains fault-controlled aquifers with the media of discrete fracture, dual porosity, cavity and dual permeability but not fractured continuum, as in this study (Caine et al., 1996) the evolution of fault architecture is controlled by the driven force of crust without weathering.

Weathering plays an important role in the formation of a fault zone to be a good aquifer when the country rocks are of low permeability. In many cases in South Africa, these country rocks include quartzite, mudstones, shale, lava, etc., where the strongly weathered depth of these rocks might be merely a few meters but in a fault zone it could be tens of meters or hundreds of meters. This linear weathered zone is often a preferable target for borehole siting and groundwater development.

Groundwater exploration results along the Taaibos fault from the farms Greenfield, Ysselmonde and Rhone show that all the high yield boreholes are restricted to a zone less than 100 m wide along the fault (Fayazi and Orpen, 1989), where the damage zones consist

of Karoo sedimentary rocks in the north and Letaba basalt in the south (Fig. 16). Moreover, geophysical surveys and exploration core logging also confirmed a weathered zone material along the fault line as the target of production borehole siting. According to Fayazi and Orpen (1989), these boreholes were never drilled to a depth in excess of 80 m.



Figure 16 Map showing the Taabos fault and boreholes drilled in the Alldays area

4.3.2 Composite groundwater barrier/conduit – discrete fracture model

In a discrete fracture model, fractures are explicitly represented and the matrix can be assumed to be impermeable (National Research Council, 1996). A discrete fracture model requires data on the geometry and hydraulic properties of individual fractures. Such data are almost always far from complete for a given field site and very few studies have depicted the field condition in order to apply the model to assess groundwater.

With respect to the aquifer of the Rawsonville site, there are three independent aquifer systems; of these, two are fractured rocks on both damage zones of the normal fault, where the west side is an artesian flow system and the east a non-artesian flow system. Another aquifer system is the shallow groundwater flow through the boulder soil and regolith, fed by the stream water running through the site. At the initial stage of borehole construction in

2006, there was no linkage between the shallow and deep groundwater systems. However, from the field work in 2013, it was observed that due to the flooding, the stream water has often fed the non-artesian boreholes of which the water level in borehole BH-2 was around 0.3 m above ground level. These observations, together with the additional field survey and borehole loggings, not only help to obtain a better understanding of the fault-controlled aquifer, but also to establish a site-specific conceptual model which is presented in Figure 17 with the plan view in Figure 3.

In this site, results of borehole core logging and observation of hydraulic tests have confirmed that the fault core with a width of 80 m acts as a groundwater barrier, namely there is no communication between the groundwater in both damage zones (Lin, 2008).

- The fault core consists of highly fractured cataclasites, cemented by secondary minerals, abating the porosity of fault core material and connectivity of the fracture.
- The fault core separates the fractured rock into an unconfined aquifer in the hanging wall where groundwater occurs with static water levels and a confined aquifer in the footwall where groundwater appears as an artesian flow.
- It is observed that in both fractured aquifers the conductive zones intercepted by the boreholes are not at the fault core but at its fracture zones of the fault. The evidence confirms the conceptual model proposed in Table 4.

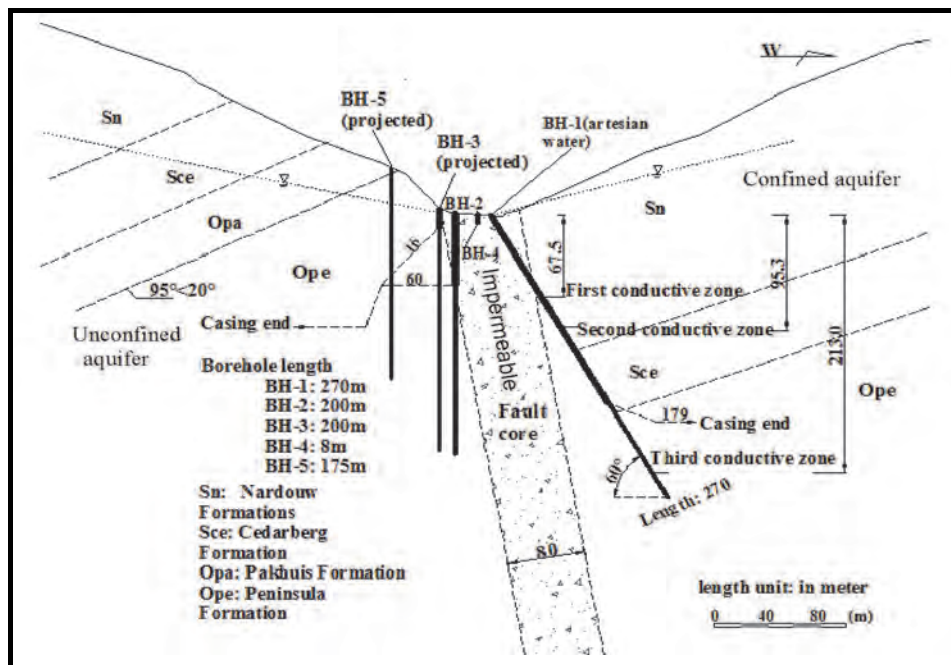


Figure 17 Hydrogeological conceptual model of a fault-controlled aquifer at the Rawsonville site

5 NUMERICAL MODELLING

5.1 Purpose and scope

Because the subsurface aquifer media are not easily observed, various models have become the tools employed to understand groundwater systems via simulating and predicting their behaviors (Water Science and Technology Board, 1990). Models are often used to physically simplify a complex system and mathematically represent key phenomena of the system (Chiang and Kinzelbach, 2001; Anderson and Woessner, 2002). In terms of groundwater management, it is necessary to conduct numerical modelling for the resource evaluation. Compared with analytical methods, numerical modelling provides a fast and sometimes effective way to evaluate bulk behavior and the quantity of groundwater resources (Sophocleous and Devlin, 2004).

Current three-dimensional numerical modelling is based on either the finite-element or finite-difference model codes to simulate steady or transient flow of groundwater with uniform density (Van Heeswijk and Smith, 2002). The model is largely calibrated to the monitoring data including water level, natural or artificial discharge, groundwater recharge, the change of boundary condition over time, etc. The model applicability is dependent on a sound establishment and refinery of the aquifer conceptual model.

The purpose of this section is to evaluate how groundwater flows along a fault where the fault core is impermeable in light of data derived from field work at the Rawsonville site, which includes core logs of boreholes BH-1 and BH-2 and the observations during hydraulic tests (Lin, 2008). In the case of the five borehole network at the site, it is of necessity to determine the scope of aquifer and evaluate how the hypothetical scenarios of future abstractions would affect the groundwater flow system.

Based on the analytical results of site measurement and aquifer characterization and conceptualization, we are now able to refine the initial conceptual model as discussed before and produce a sound conceptual model for the site-specific groundwater problem. In this study, we use the software Feflow 6.0 with model codes on a basis of finite element method to:

- 1) Simulate natural groundwater flow on the damage zone by characterizing the distribution of the aquifer hydraulic head;
- 2) Examine the effects of pumping alternatives on the resource concentration;
- 3) Determine the possible travel time of potential pollutant drive by the flow process;

- 4) More importantly, for groundwater management purposes, determine the sustainable yield through analyzing the impact of groundwater abstraction on the change of groundwater resource quantity.

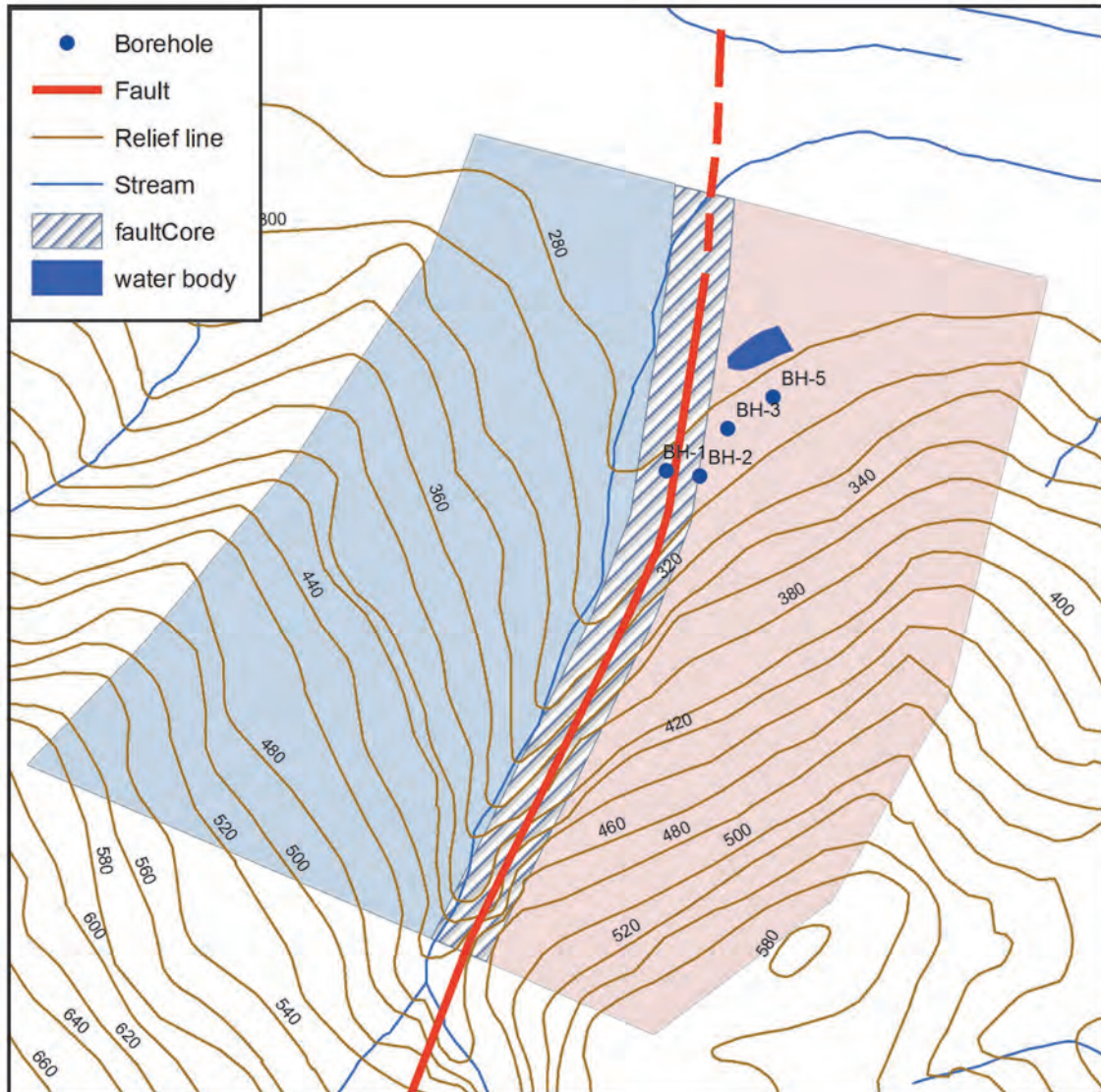


Figure 18 Initial model area of the Rawsonville site

5.2 Model configuration and data process

5.2.1 Hypothesis

It is assumed that at the Rawsonville site, groundwater occurs in the fractured damage zones, but not the fault core. This suggests that the hydraulic properties of the fault core can be assigned as nil. However, during the simultaneous simulation of groundwater flow on both fault damage zones (Fig. 18), an advance simulation result showed that the fault core

somehow continued to dewater while the water levels rose in both zones. Moreover, field observation has evidenced that the aquifer in the west damage zone is a typical fracture flow system and the current model is perhaps unsuitable to evaluate the type of flow. These lead to the following hypotheses:

- (1) The confined aquifer in the west, with groundwater originating from a single conductive zone (Fig. 17); and an unconfined aquifer in the east which is closely connected to the surface water system.
- (2) Fault core, in this case, is an impermeable body with hydraulic properties of nil.
- (3) Aquifers of both damage zones cannot be simulated at the same time.

Thus, in recognition of the independent groundwater flow system on each side of the fault, in this study only the unconfined aquifer in the east is extracted for the modelling process.

5.2.2 Surface water/groundwater interaction

It is assumed that the dominant mechanism for the discharge of groundwater from the system is through the river bed and via spring flows to the rivers and that the river and groundwater are in dynamic connection. Based on this assumption, it is possible at the modelling stage to use the observational result on the stream which perennially runs through the site area with the stream bed roughly riding along the fault core. Additional groundwater flow information collected by Nel (2011) showed that the borehole flow changed seasonally due to the interaction between groundwater and the stream and precipitation.

5.2.3 Model preparation

The model area is shown in Figure 18, the east part of the fault core. The size of the area is 1 500 m (north-south) by 500 m (north-south) or 0.7 km², with elevation ranging from 275 m in the north to 570 m in the south. The model area is defined to fit the groundwater problem studied at a site scale. Furthermore, considering the constraint of damage zone width, its east boundary is defined to be along the slope divide, which will be discussed later.

The development of the model is based on the conceptual understanding of the aquifer, as has been discussed in a previous section. To establish a conceptual model, first, relevant geometrical data which include the area extent, borehole position and depth, digital elevation model, etc. are necessary. All the geometrical data, including polygons and points and lines are prepared with the same projection in ArcGIS because they can be directly recognized by the Feflow as the software is flexible in the spatial discretisation. For example, the surface

topographical data is extracted from the site DEM and then converted into a relief point table before it is loaded up and integrated after model discretization by the modelling software.

Figure 19 shows the discretized initial conceptual model on the left and associated model geometry on the right where there are 6 988 mesh elements and 4 640 mesh nodes in total and in the vicinity of the borehole and model boundary the mesh element density is enhanced. It is noted that the model is divided into four layers, in light of possible changes in aquifer hydraulic properties at depth according to the result from previous packer tests conducted in borehole BH-2 (Lin, 2008). The model bottom is defined by the bottom of borehole BH-3 with a total length of 200 m. With this initial conceptual model, it is possible to specify other modelling data such as hydraulic boundary conditions, the initial water head and aquifer hydraulic properties.

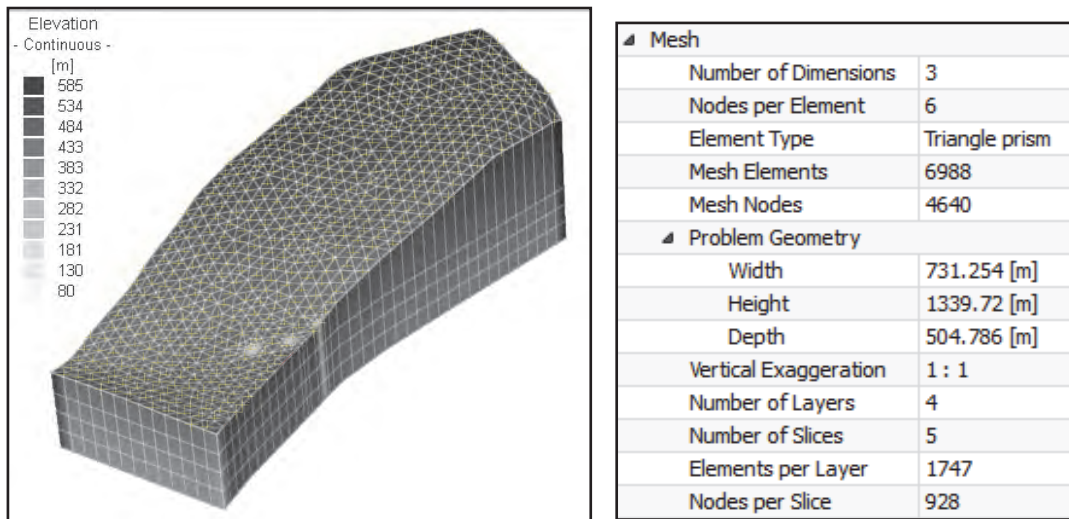


Figure 19 Model configuration

5.3 Boundary condition

5.3.1 Model boundary

By default, the model takes all the nodes on the model boundary to be an inactive or no flow boundary. It is critical to define the model geometric/physical boundary and subsequently determine the model scope in three dimensions.

- Model bottom

As the model is built to fit the groundwater condition on a site scale, its bottom is defined by the bottom of borehole BH-3 with a total whole length of 200 m.

- West boundary

The fault core, where hydraulic properties are assumed as nil, naturally forms a boundary with inactive mesh nodes on the four layers' borders.

- North boundary

The northern boundary is defined by the stream which is topographically the lowest zone of the model area. According to the result of borehole and stream levelling, the stream level at the northern boundary is around 280 m amsl.

- South boundary

The south boundary is topographically restricted to the first 40 m high waterfall on the stream with perennial flow. Geologically, the throw of the fault seems to be drastically reduced. It is hence assumed that the aquifer on the damage zone in both geometry and hydrogeological properties may also change, which separates the site aquifer from the others along the fault zone.

- East boundary

Physically, there is no evidence to define the east boundary. According to previous studies conducted in brittle rock formations (Gudmundsson and Geyer, 2006; Johri, 2012), there is generally a close relationship between the thickness of the fault damage zone and displacement. Using fault throw to represent the displacement, Shipton and Cowie (2001; 2003) estimated that the thickness of the fault damage zone is around two and a half times that of the fault throw, based on their research of the evolution of faults at a meter to kilometer scale on brittle sandstones.

The above method may be adapted to the case of the fault developing in the TMG sandstone. Through the examination of borehole core of BH-1 and surface landform which indicates the bottom of the Cedarberg shale, the fault throw near the groundwater site is about 180 m to 250 m but that value reduces to the south (Fig. 2). Therefore, the thickness of the fault damage zone for this modelling is estimated as 500 m; this forms the basis of the eastern no flow boundary determination.

5.3.2 Hydraulic head

Unlike the other groundwater modelling, the hydraulic head in Feflow is defined as the head for the model process (such as initial head) and hydraulic boundary conditions. It is assumed that under natural conditions, the inflow to the system as the groundwater recharges and the outflow from the system as groundwater discharges are directly controlled by the stream and located on the west corners of both the south and north boundaries, as shown in Figure 20, with the associated hydraulic head, as shown in Table 6. A constant head at either boundary may be assigned to the nodes where the stream in reality is located to start with this simulation.

The imposition of the constant head boundary around the model area (Fig. 20) is based on the assumption that the groundwater flow system in the model area is relatively independent. This simplifies the interaction between surface water and groundwater within the modelled area, which allows for the flux exchange between the local groundwater flow system and the outside.

From the observed water levels of boreholes BH-2, BH-3 and BH-5, the hydraulic head in this borehole has changed over time since the drilling was completed in 2006. For example, the initial water level of 2.5 m blg in BH-3 was recorded in 2007 but 0.9 m blg in October 2013; the same trends were observed in BH-2 and BH-5. Therefore, an average value of the water levels for each borehole is assigned for the model process hydraulic head. The time drawdown observations have confirmed that the groundwater in the three holes is connected with one other. In the case of future pumping in BH-3 or BH-5 with different alternatives, thereby in the simulation of a pumping condition in this area, boreholes BH-3 and BH-5 could not be assumed as initial head boundaries. Borehole BH-2 is taken as a head boundary (Fig. 20).

Table 6 Boundary and initial condition for model simulation

Site		BH1	BH2	BH3	BH4	BH5	Stream
Ground elevation (m)		286.825	285.924	283.341	284.634	284.983	
Water level (m)		287.30	283.92	282.24		283.18	
Boundary condition (m)	North						281.00
	South						291.00
	Well						
Model process hydraulic head			head 1				

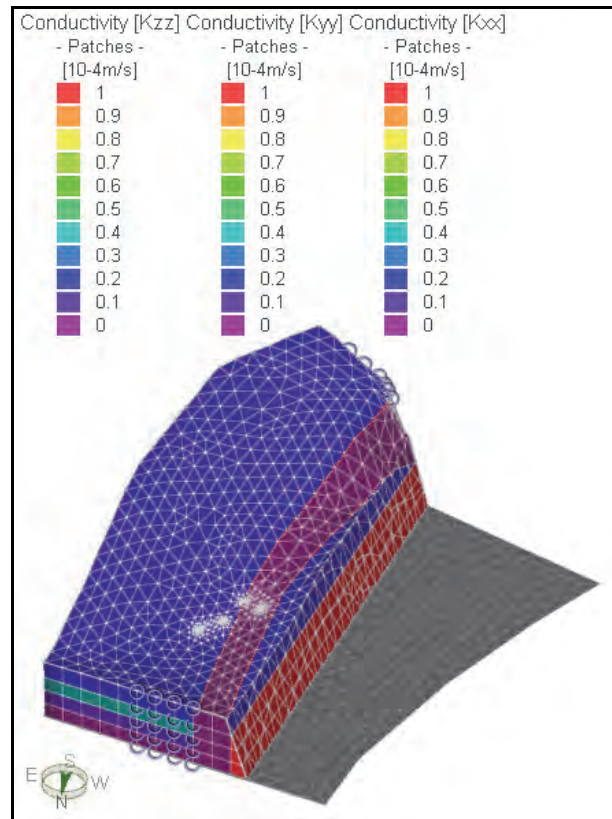


Figure 20 Conceptual model with the distribution of hydraulic conductivity assigned to the layers

5.4 Model processing

5.4.1 Hydraulic properties

Besides a better understanding of the aquifer hydrogeological setting and a realistic conceptual model, the determination of aquifer hydraulic properties is essential for a numerical model. In fractured rocks, the anisotropy in both material and hydraulic properties is not an uncommon phenomenon. In order to conduct meaningful modelling, it is necessary to have the assumption that the groundwater is flowing through a geological continuum, or the aquifer may be simplified into a fractured porous media. Because both site-scale pumping tests and borehole-scale packer tests determine the bulk aquifer hydraulic properties, and because the groundwater links each of the boreholes, this unconfined aquifer can be regarded as an aquifer with fractured porous media.

In 2006 and 2013 a number of pumping tests were conducted in boreholes BH-3 and BH-5, and in October 2013 a constant head test was done in borehole BH-1, resulting in a range of hydraulic properties K and S values. During coring, hole drilling packer tests were carried out in both boreholes BH-1 and BH-2. The hydraulic conductivity derived from the pumping tests

falls in a range of 10^{-5} to 10^{-7} m/s, but the packer test gave a range from 10^{-2} to 10^{-5} m/s. Moreover, the hydraulic conductive estimated by the hydraulic tensor method by using the three-dimensionally interconnected fractures (Lin, 2008) is in the order of a magnitude of 10^{-6} m/s.

To perform the modelling and associated analysis in the fractured porous media aquifer, we assume that aquifer parameters of a layer in a horizontal (x, y) direction are uniform but not in a vertical (z) direction. Considering the change of hydraulic conductivity at depth (Fig. 21), the K values are assigned on a layer basis with $K_x=K_y$ but $K_z=0.5K_x$. Based on the result of pumping tests and packer tests, the K values decided on for input in the model is listed in Table 7 and shown in Figure 20.

Table 7 Layer elevation and associated hydraulic conductivity and specific storage

Layer No.	Bottom elevation (m)	$K_x=K_y$ (m/s)	K_z (m/s)	S
1	230	1.90E-05	9.50E-06	1.2E-04
2	180	5.70E-05	2.85E-05	2.0E-05
3	130	9.80E-06	4.90E-06	9.5E-06
4	80	8.00E-07	4.00E-07	1.7E-07

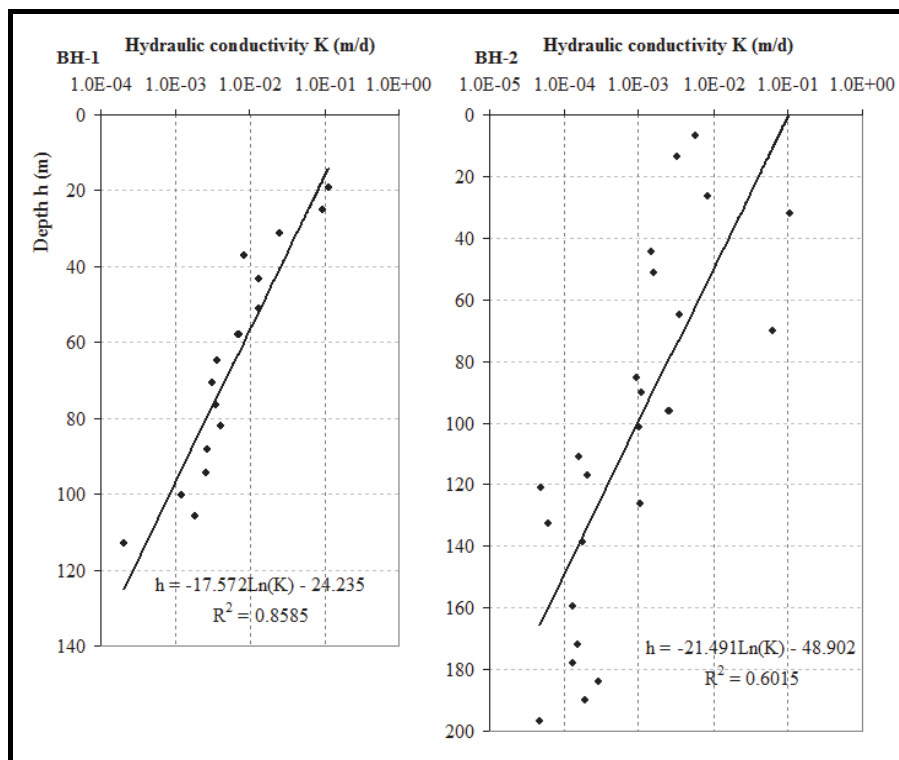


Figure 21 Hydraulic conductivity plot against depth from packer tests in BH-1 and BH-2 at the Rawsonville site (after Lin, 2008).

5.4.2 Model processing

By using the above data input, it is possible to simulate the natural condition of groundwater flow in an unconfined environment. During this process:

- A 10 year time period is used to simulate the flow with maximum iteration of 12 steps being included in each period in the model calibration process.
- In the four layer model domain, elevation of the first layer ranges from the surface to 230 m amsl. This implies that the layer might be partially dewatered in the case of well abstraction. Therefore, a free and movable water table is assigned to the model layer.
- In the modelling process, the forward prediction corrector scheme is set up for the groundwater problem.
- Because the model domain water budget is checked in an advance modelling, the change of hydraulic head will be the major parameter that we extract and discuss in the study.

5.4.3 Simulation result and discussion

5.4.3.1 Natural flow

The unconfined groundwater with a transient state is used to simulate the natural groundwater flow with the hydraulic gradient initially defined by the observed water levels.

- As can be seen during model running, the state of equilibrium over the groundwater domain was attained within 1 900 days or 5.28 years. The migration of the water body starts at the hydraulic boundary and the initial head area as the flow is controlled through actual hydraulic heads.
- The simulated hydraulic head is shown in Figure 22, where the isoline of the head indicates a horizontal direction of flow which is from the south to the north.
- Figure 22 also shows the recharge area with the natural hydraulic head located at the area of more than 285 m amsl, while the boreholes are located on the major flow path near the top of the discharge area.
- Comparing the simulated hydraulic head with the observed ones (Table 8), it is noted that, except for borehole BH-3, the error of hydraulic head BH-5 and BH-2 seems acceptable. This implies that the conceptual model is well refined. However, the error

would perhaps be attributed to the iteration errors arising from model configuration, or the fact that both BH-2 and BH-3 are very close to the fault core which is actually inclined to the west with a dip of 60° , but in the model it is treated as a vertical surface by the model.

- Taking into consideration the geometry of the model domain and the location of initial and constant heads as discussed in the part on the Boundary Condition, the hydraulic gradient of the modelling domain can be regarded as a constant gradient. Therefore, the flow process shown in Figure 23 might be used to roughly estimate the travel time of transport driven by the flow process, which is estimated at around the 1 900 days it would take to complete a transport process. However, whether or not this result can be used as the input for geochemical modelling, more detailed study would be required.

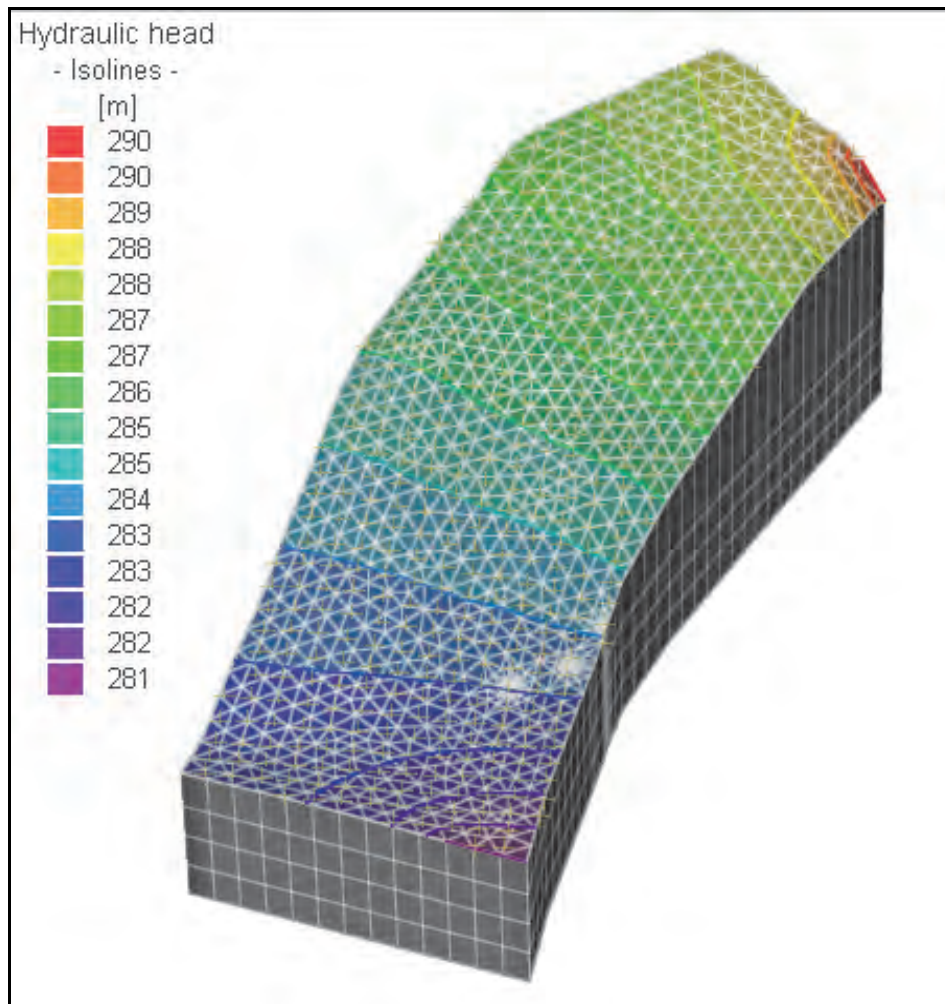


Figure 22 Modelling result with a balancing water table collectively calibrated by initial and boundary conditions in an unconfined environment

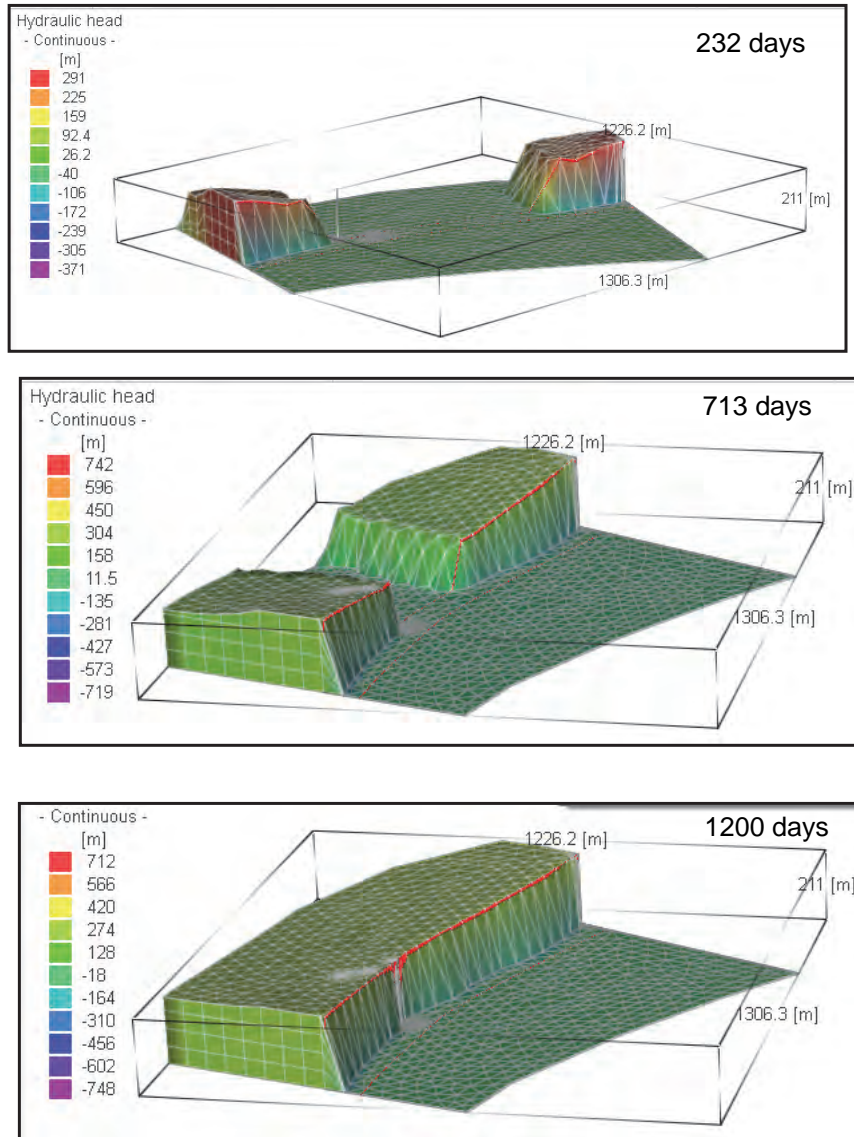


Figure 23 Model used to estimate the travel time driven by the flow process

Table 8 The comparison of the measured water level and simulated water level

Borehole	Observed WL (m amsl)	Simulated WL (m amsl)	Error (%)
BH-2	283.92	284	2.8
BH-3	282.24	284	6.2
BH-5	283.18	283	0.6

5.4.3.2 Groundwater abstraction and sustainable yield

The groundwater quality of the above mentioned aquifer is generally good as has been discussed before. Because the well field with a five borehole network was initially developed as a monitoring and research base, it has not yet experienced any continuous groundwater abstraction for water supply. However, as one of the resource options for a dry season, it is necessary for the different options of groundwater management to be assessed. One of the key issues of groundwater management is the determination of a sustainable yield.

In this study, a number of pumping scenarios are set up to examine the impact of groundwater abstraction on the capture zone and to determine an option of sustainable yield for the specific aquifer.

(1) Pumping scenarios

Groundwater recharge is assumed to be constant, which is defined by the hydraulic boundary conditions in the model. This ensures that the aquifer has a sustainable supplement to the capture zone when the borehole is continuously pumped. There are two deep percussion holes at the site; in this case only borehole BH-3 is selected to simulate the pumping process at a pumping rate of 15 ℓ/s and 20 ℓ/s , respectively. The simulation results are shown in Figure 24 to Figure 27 and summarized as follows:

- The stabilized drawdown at a pumping rate of 15 ℓ/s is 38 m and for 20 ℓ/s the pumping rate is 53 m.
- Time to arrive at a stable water level depends on the pumping rate; in this case the lower the pumping rate, the faster for the water table to be stabilized.
- The cone of depression on the fault zone seems to be time dependent and restricted to a half circle. Furthermore, the development of a depression cone slowly changes the original groundwater dynamics as the flow direction is gradually predominated by the pumping well.
- Figure 27 shows the result of a five day or 1 780 hour simulated pumping test at BH-3, from which the bulk hydraulic properties can be inversely estimated. This sheds light on the inverse estimation of hydraulic properties for further model calibration.

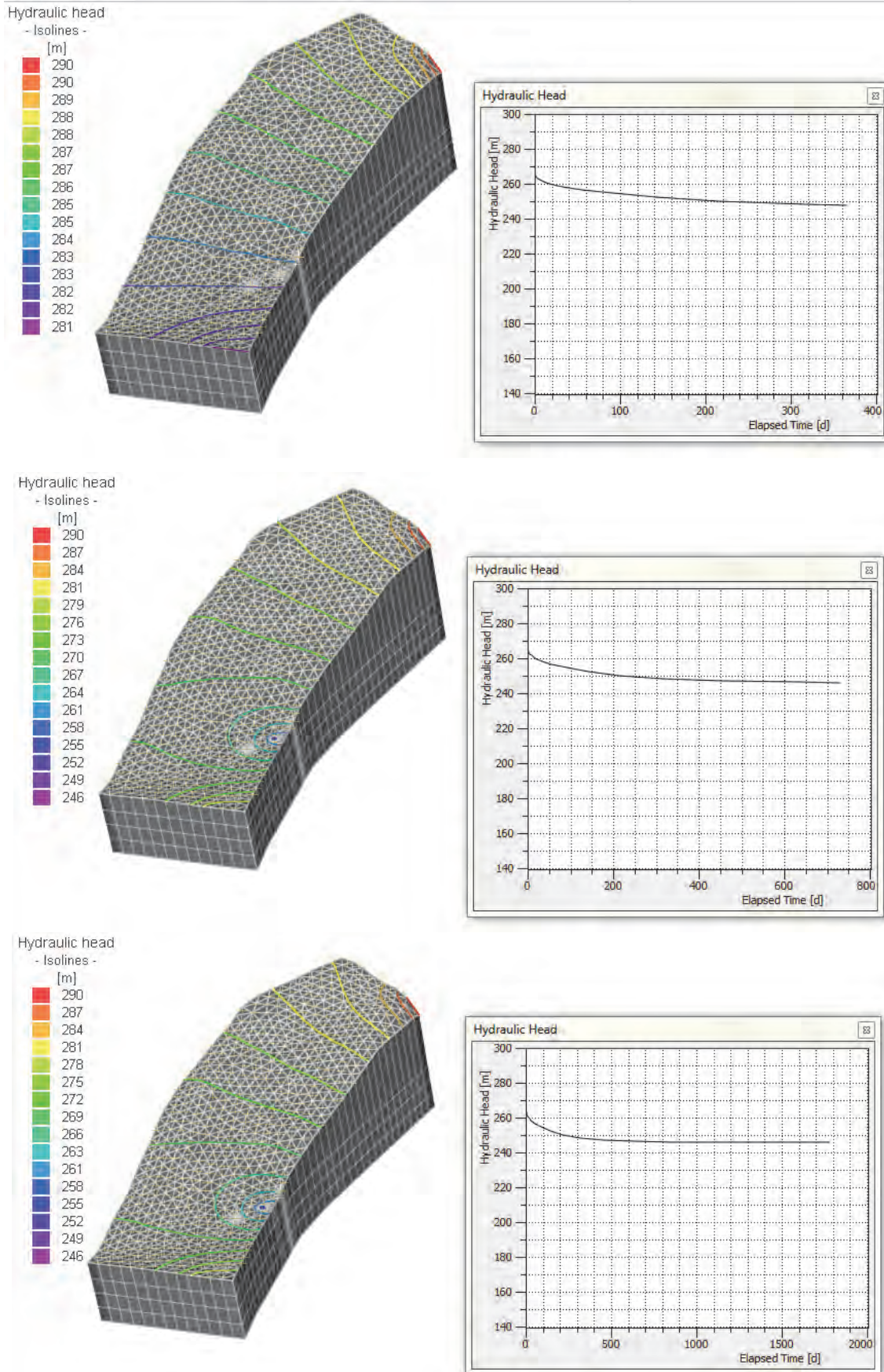


Figure 24 Effect of abstraction on the hydraulic head in BH-3 at flow of $Q=15$ l/s

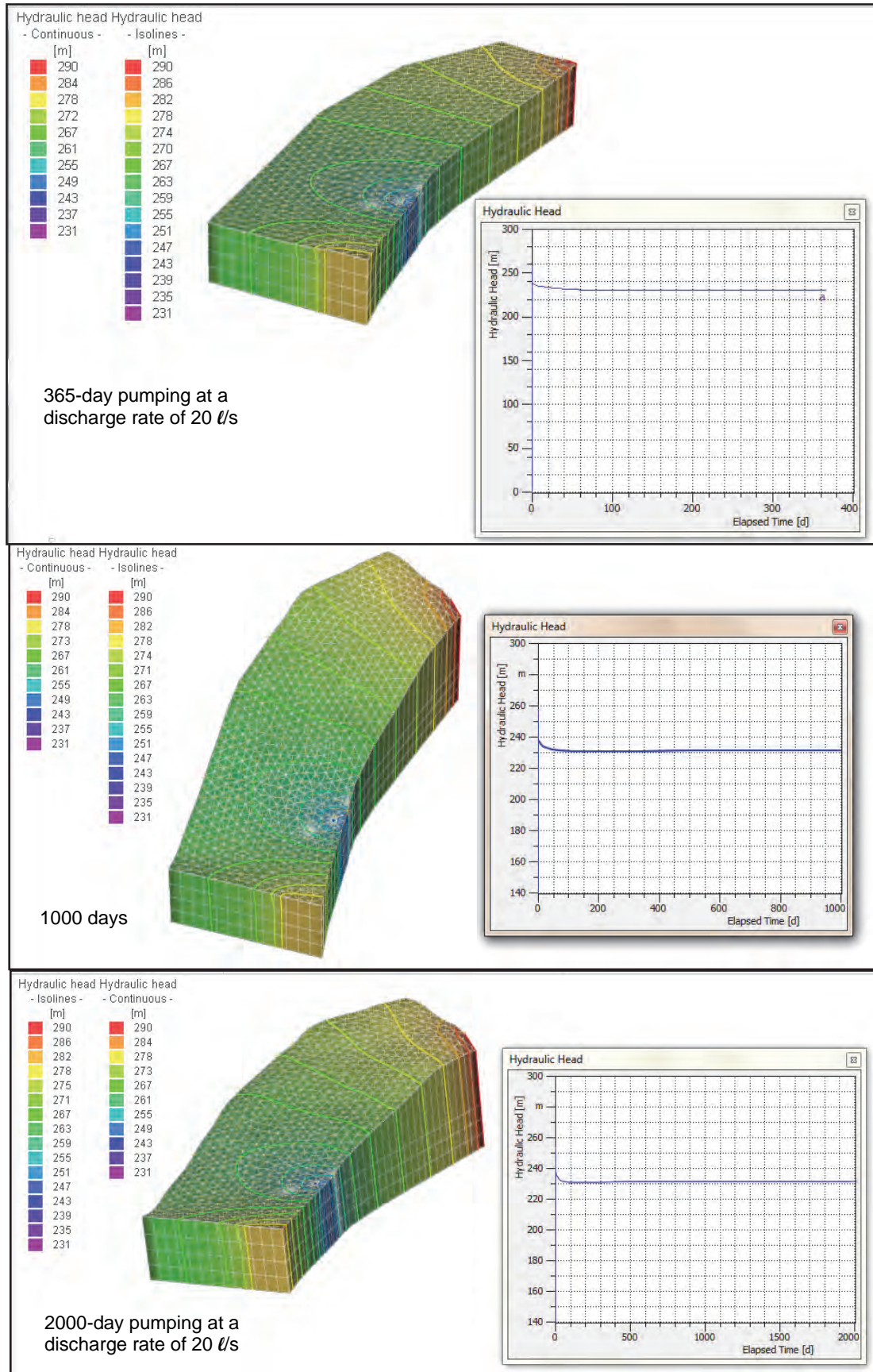


Figure 25 Effect of abstraction on the hydraulic head in BH-3 at a flow of $Q=20 \text{ l/s}$

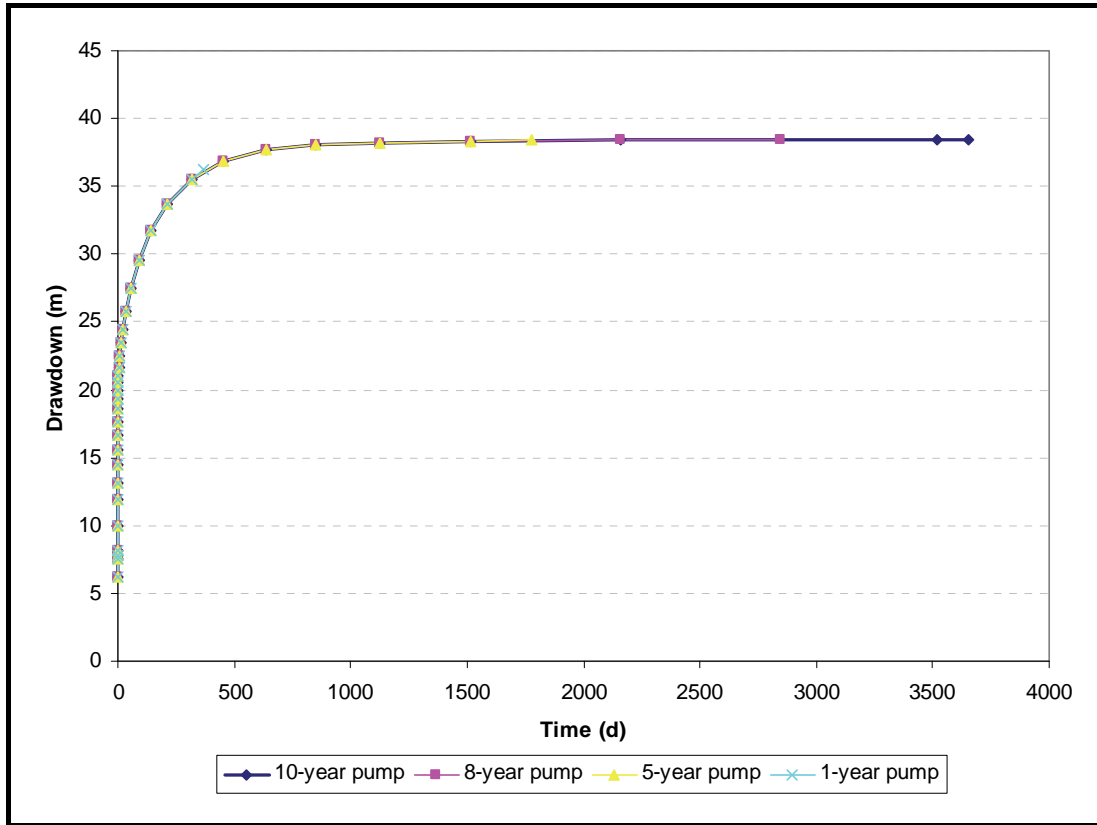


Figure 26 Drawn from long term well abstraction at the flow rate of 15 ℓ/s

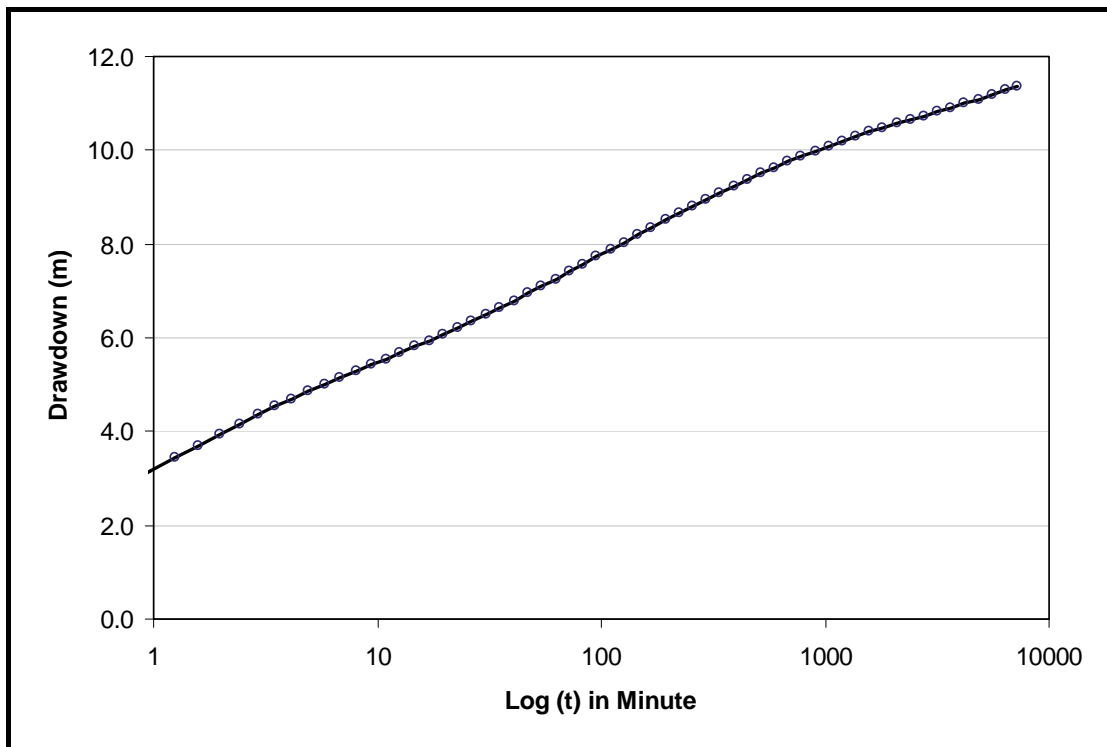


Figure 27 Drawdown time curve derived from a simulated pumping test with a duration of five days (1 780 hours) and a flow range of 8 ℓ/s at BH-3

(2) Determination of sustainable yield

The concept of sustainable development was proposed in the 1980s, which forced a reconsideration of safe yield practices. Alley et al. (1999) defined groundwater sustainability as the development and use of groundwater in a manner that the water can be maintained for an indefinite time without causing unacceptable environmental, economic or social consequences.

In the past in South Africa, sustainable yield used to be determined by groundwater recharge, viz. the total amount or percentage of recharge. Seward et al. (2006) pointed out that groundwater sustainable yield is dependent on the amount of capture. Whether or not this amount is socially acceptable is a reasonable compromise between little or no use, on the one extreme, and sequestration of all natural discharge, on the other extreme (Ponce, 2007). This requires a policy for the compromise between the governmental authority and groundwater user.

As can be seen in Figure 24 to Figure 26, along with pumping continuing, the water table will anyway arrive at a stable level; the time for the water table to be stabilized depends on the pumping rate. From this point of view, the sustainable yield of a specific aquifer seems to be a dynamic amount. Technically, it can be determined by the prescriptive water table without causing a costly pumping experience, and by the deterioration of adjacent groundwater and the ecological environment.

In order to determine the sustainable yield for this research site, the aquifer simulation at multiple pumping rates ranging from 2 ℓ/s to 25 ℓ/s and with all the durations of 10 years was performed. Considering the top portion of the aquifer that might be dewatered by the higher well discharge, the simulated pump was installed at the lower part of the aquifer, viz. layers 3 and 4. Data of the hydraulic head and time duration were extracted after a pumping scenario was completed. The modelling results for the relationship between drawdown and time are shown in Figure 28, where due to various pumping rates the minimum stable drawdown is 4.9 m and the maximum drawdown is 76.8 m which are stabilized in 500 days to 1 500 days.

For the determination of sustainable yield, the relation of stabilized drawdown (s_w) and pumping rate (Q_a) is established as shown in Figure 29. By using the curve fitting, we have the following formula to represent the relation of s_w and Q_a :

$$s_w = 2.2189 \cdot Q_a^{1.0653}$$

This provides an option for the groundwater user to make an informed decision. The question of how to pump sustainably depends on the compromise between the groundwater user and governmental authority. Based on the understanding of the aquifer setting and potential recharge, the maximum stable drawdown is recommended as not more than 20 m. Therefore, the recommend amount for the pumping rate is $Q_a=4 \text{ l/s}$ to 7 l/s , with a corresponding drawdown of 9.7 m to 17.6 m.

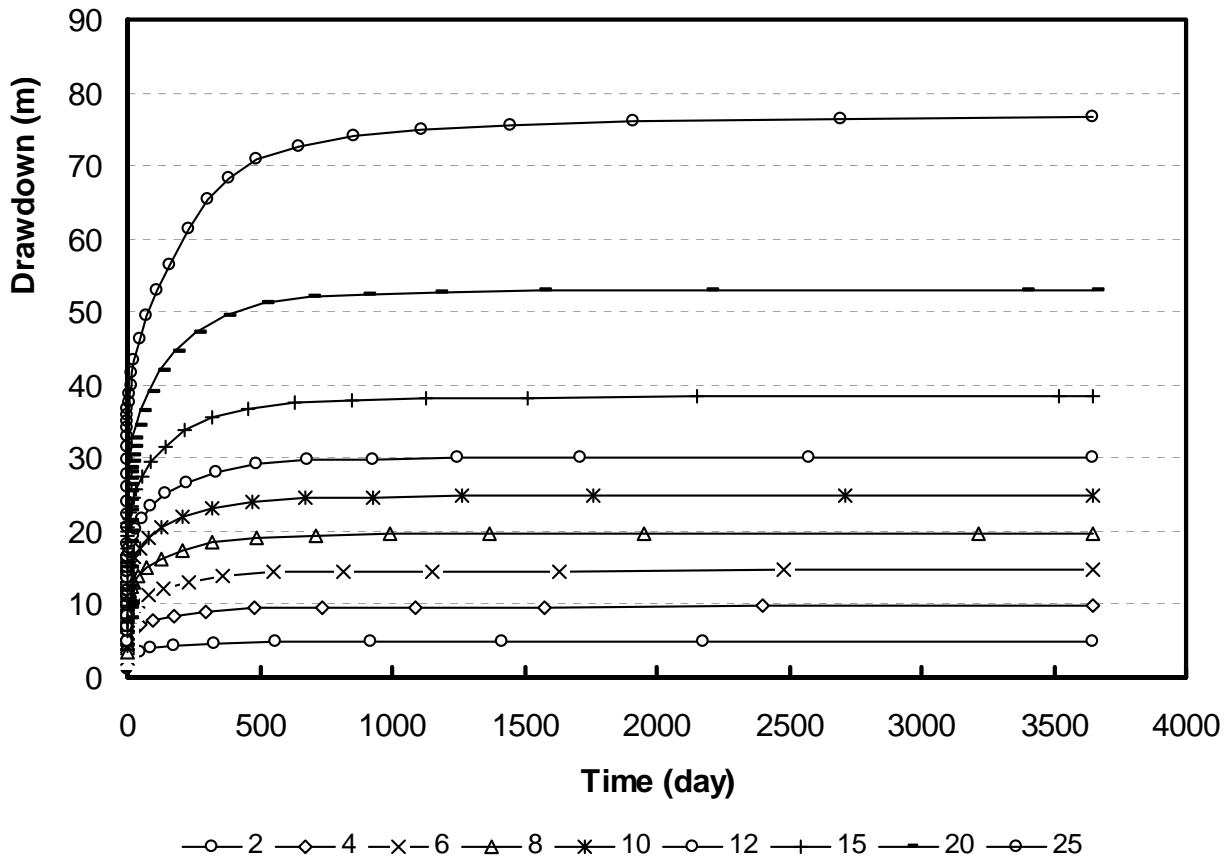


Figure 28 Simulated drawdown by a 10 year well abstraction at various pumping rates

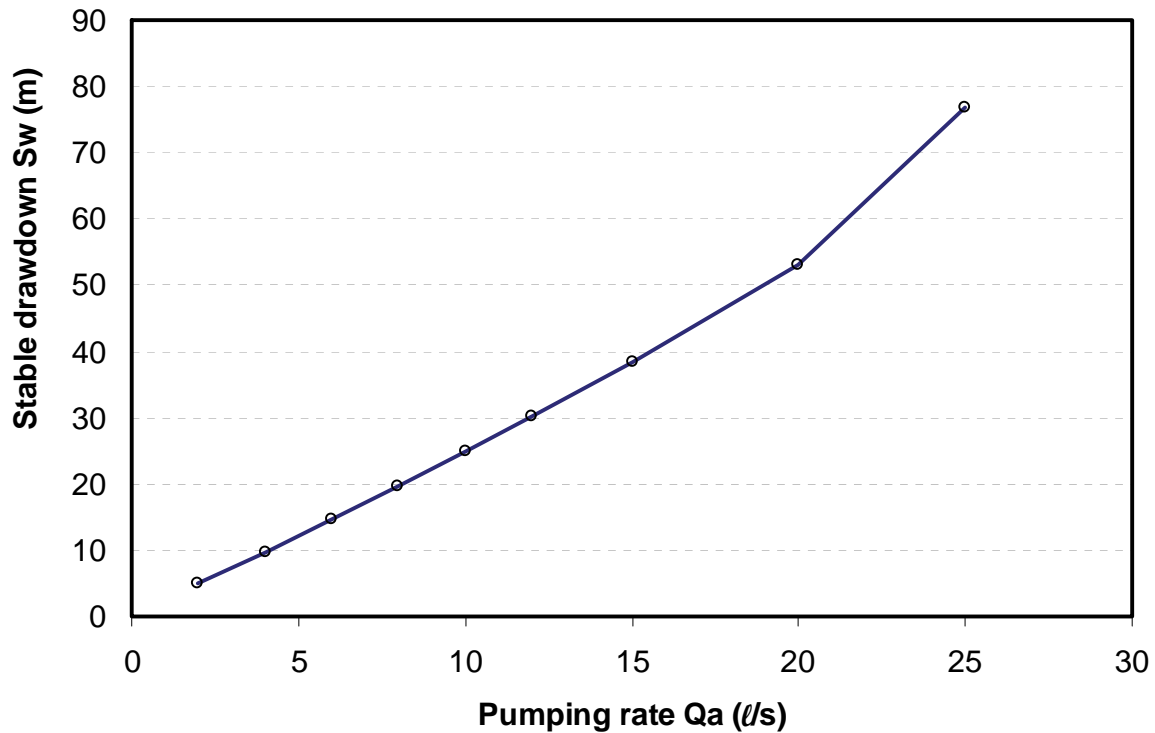


Figure 29 Relationship between pumping rate and stable well drawdown

5.5 Summary

Groundwater numerical modelling provides an effective way towards the evaluation and prediction of groundwater behavior and quantity. A three dimensional modelling was performed in this study for the fault controlled aquifer at the Rawsonville site, using Feflow (Version 6.0). The modelling process started with the conceptual model and with an understanding derived from drilling, field measurements and hydraulic tests, attempts are made to:

- Simulate natural groundwater flow on the damage zone by characterizing the distribution of the aquifer hydraulic head;
- Examine the effects of pumping alternatives on the resource concentration;
- Determine possible travel time of potential pollutant drive by flow process;
- Determine the aquifer sustainable yield through analyzing the impact of groundwater abstraction on the change of groundwater levels.

In this study, the natural flow system and flow with pumping scenarios were simulated, respectively. Results for the natural flow system show that balancing groundwater dynamics with groundwater in the fault damage zone flowing from the south and discharging in the north, while the four borehole network is located on the upper part of the discharge area; the simulated water level is well correlated with the observed water levels at the boreholes.

Simulated results with different pumping alternatives show a distinct impact of groundwater abstracting on the hydraulic head. Continuous pumping may change the original groundwater dynamics reflected by a change in flow direction and the development of depression cones on the damage zone. Long term abstraction slowly increases the well drawdown but it would stabilize at a certain level which is dependent on the pumping rate.

To estimate the aquifer sustainable yield, a relationship between simulated drawdown and pumping rate was established which is represented by:

$$s_w = 2.2189 \cdot Q_a^{1.0653} \text{ where } s_w \text{ is the drawdown and } Q_a \text{ the pumping rate.}$$

This empirical relation derived from the site specific study provides an option for informed decision making. Issue of how to sustainably pump might rely on the compromise between the groundwater user and governmental authority. Based on the understanding of the aquifer setting, the maximum stabilized drawdown is recommended as not more than 20 m. Therefore, the recommended amount for the pumping rate was estimated at 4 ℓ/s to 7 ℓ/s , with corresponding drawdowns of 9.7 m to 17.6 m, respectively.

6 REFERENCES

- Ahmadov, R., Aydin, A., Mohammad, K.-F. and Durlofsky, L.J., 2008. Permeability upscaling of fault zones in the Aztec Sandstone, Valley of Fire State Park, Nevada, with a focus on slip surfaces and slip bands. *Hydrogeology Journal*, DOI 10.1007/s10040-007-0180-2.
- Alley, W.M., Reilly, T.E. and Franke, O.E., 1999. Sustainability of groundwater resources. U.S. Geological Survey Circular 1186, Denver, Colorado, 79 pp.
- Anderson, M.P. and Woessner, W.W., 2002. Applied groundwater modelling: simulation of flow and advective transport. USA, Elsevier.
- Andreoli, M.A.G., Doucoure, M. and Van Bever Donker, J., 1996. Neotectonics of Southern Africa – a review. *Africa Geoscience Review*, Vol. 3, No. 1, pp. 1-16.
- Andreoli, M.A.G., Doucoure, M., Van Bever Donker, J., Faurie, J.N. and Fouché, J., 1995. The Ceres-Prince Fabric (CPEF): an Anomalous Neotectonic Domain in the Southern Sector of the African Plate. Centennial Geocongress, Extended Abstract, Vol. I, pp. 434-437, ISBN: 0-620-19031-0.
- Antonellini, M. and Aydin, A., 1994. Effect of faulting on fluid flow in porous sandstones: petrophysical properties. *American Association of Petroleum Geologists, Bulletin* 78, pp. 355-377.
- Aydin, A., 2000. Fractures, faults and hydrocarbon entrapment, migration and flow. *Marine and Petroleum Geology*, 17, pp. 797-814.
- Bensen, V.F. and Van Balen, R., 2004. The effect of fault relay and clay smearing on groundwater flow patterns in the Lower Rhine Embayment. *Basin Research*.
- Caine, J.S., Evans, J.P. and Forster, C.B., 1996. Fault zone architecture and permeability structure. *Geology*, 24, pp. 1025-1028.
- Caine, J.S. and Forster, C.B., 1999. Fault zone architecture and fluid flow: insights from field data and numerical modelling. In: Haneberg, W.C., Mozley, P.S., Moore, J.C. and Goodwin, L.B. (Eds), *Faults and Subsurface Flow in the Shallow Crust*. AGU Geophysical Monograph, 113, pp. 101-127.
- Chevallier et al., 2009. Flow conceptualization, recharge and storativity determination in Karoo aquifers, with special emphasis on the Mvimvubu-Keiskamma and Mvoti-Mzimkhulu Water Management Areas in the Eastern Cape and KwaZulu-Natal Provinces of South Africa. WRC Project K1565, Final Report.
- Chiang, W.H. and Kinzelbach, W., 2001. 3D groundwater modeling with PWWIN. Springer, Berlin, 346 pp.
- Coronado, M. and Ramírez-Sabag, J., 2008. Analytical model for tracer transport in reservoirs having a conductive geological fault. *Journal of Petroleum Science and Engineering*, 62, pp. 73-79.

- Dustay, S. and Nel, J.M., 2013. Implementation of protection zoning. 13th Biennial Groundwater Division Conference, September 2013, Durban.
- Elhag, A.B. and Elzien, S.M., 2013. Structure controls on groundwater occurrence and flow in crystalline bedrock: a case study of the El Obeid area, Western Sudan.
- Fayazi, M. and Orpen, W.R.G., 1989. Development of a water supply for Alldays from groundwater resources associated with the Taaibos fault. Department of Water Affairs, GH Report No. 3634, May 1989.
- Ferris, J.G., Knowless, D.B., Brown, R.H. and Stallman, R.W., 1962. Theory of aquifer tests. US Geological Survey, Water Supply Paper No. 1536E, 174 pp.
- Gudmundsson, A. and Geyer, A., 2006. Effects of damage-zone thickness on fault displacement. Poster on TSK 11, Göttingen.
- Hartnady, C.H. and Hay, E.R., 2002. Boschklouf Groundwater Discovery, In: (Petersen, K. and Parsons, R., eds), A synthesis of the hydrogeology of the TMG formation of a research strategy. WRC Report No. TT 158/01, pp. 168-177.
- Hälbich, I.W. and Greef, G.J., 1995. Final report on a structural analysis of the west plunge nose of the Kammanassie anticline. Technical Report to SA DWAF.
- Johnson, M.R., Anhaeusser, C.R. and Thomas, R.J. (ed.), 2006. Geology of South Africa. Council for Geoscience, 691 pp, ISBN: 1-919908-77-3.
- Johri, M., 2012. Fault damage zones – observations, dynamic modeling, and implications on fluid flow. PhD thesis, Stanford University.
- Karasaki, K., Freifeld, B., Cohen, A., Grossenbacherb, K., Cook, P. and Vasco, D., 2000. A multidisciplinary fractured rock characterization study at Raymond field site, Raymond, CA. Journal of Hydrology, V236, pp. 17-34.
- Kotze, J.C., 2002. Towards a management tool for groundwater exploitation in the Table Mountain sandstone fractured aquifer. WRC Report No. 729/1/02.
- Kruseman, G.P. and De Ridder, N.A., 1994. Analysis and evaluation of pumping test data. International Institute for Land Reclamation and Improvement, The Netherlands, 377 pp.
- Kulatilake, P., Jeong-gi, U., Wang, M., Escandon, R. and Narvaiz, J., 2003. Stochastic fracture geometry modeling in 3-D including validations for a part of Arrowhead East Tunnel, California, USA. Engineering Geology, 70, pp. 131-155.
- Lin, L., 2008. Hydraulic properties of the Table Mountain Group (TMG) aquifers. PhD thesis, University of the Western Cape.
- Maclear, L.G.A., 2001. The hydrogeology of the Uitenhage Artesian Basin with reference to the Table Mountain Group Aquifer. Water SA, Vol. 27, No. 4, pp. 499-505.
- McCathy and Rubidge, 2005, , the Story of Earth and Life, a South African Perspective on a 4.6-billion-year Journey, New Holland Publishing (South Africa): 184-211.

- McGrath, A.G., 1994. Damage zone geometry around fault tips. *Journal of Structural Geology*, Vol. 17, No. 7, pp. 1011-1024.
- National Research Council, 1996. *Rock fractures and fluid flow: contemporary understanding and applications*. National Academy Press, Washington DC.
- Nel, J.M., 2011. Implementation and benefit of groundwater source protection in fractured rock aquifers in South Africa. PhD dissertation, University of the Western Cape.
- Newton, A.R., Shone, R.W. and Booth, P.W.K., 2006. The Cape Fold Belt, In: (Johnson, M.R., Anhaeusser, C.R. and Thomas, R.J., eds), *The Geology of South Africa*. Geological Society of South Africa, Pretoria, pp. 521-530.
- Odling, N., Harris, S. and Knipe, R., 2004. Permeability scaling properties of fault damage zones in siliclastic rocks. *Journal of Structural Geology*, 26, pp. 1727-1747.
- Petersen, K. and Parsons, R. (eds), 2001. *A synthesis of the hydrogeology of the Table Mountain Group – Formation of a Research Strategy*. WRC Report No. TT 158/01.
- Pollard, D.D. and Aydin, A., 1988. Progress in understanding jointing over the past one hundred years. *Geological Society of America Bulletin*, 100, pp. 1181-1204.
- Ponce, V.M., 2007. Sustainable yield of groundwater. <http://groundwater.sdsu.edu/>.
- Rosewarne, P.N., 1993a. St Francis Bay Groundwater Monitoring Final Report. SRK Report No. 171719/M6.
- Rosewarne, P.N., 1993b. Ceres Groundwater Investigation Phase 2: Borehole Siting. SRK Report No. 197759/1.
- Serzu, M.H., Kozak, E.T., Lodha, G.S., Everitt, R.A. and Woodcock, D.R., 2004. Use of borehole radar techniques to characterize fractured granitic bedrock at AECL's Underground Research Laboratory. *Journal of Applied Geophysics*, 55, pp. 137-150.
- Seward, P., Xu, Y. and Brendock, L., 2006. Sustainable groundwater use, the capture principle and adaptive management. *Water SA*, Vol. 32, No. 4, pp. 473-482.
- Shipton, Z.K. and Cowie, P.A., 2001. Damage zone and slip surface evolution over micron to km scales in high-porosity Navajo sandstone, Utah. *Journal of Structure Geology*, 23, pp. 1825-1844.
- Shipton, Z.K. and Cowie, P.A., 2003. A conceptual model for the origin of damage zone structures in a high-porosity sandstone. *Journal of Structure Geology*, 25, pp. 333-344.
- Sophocleous, M. and Devlin, J.F., 2004. Discussion on the water budget myth revisited: Why hydrogeologists model. *Ground Water* 40(4), pp. 340-345.
- Stamos et al., 2003. *Geologic setting, geohydrology and ground-water quality near the Helendale fault in the Mojave River Basin, San Bernardino County, California*. U.S. Geological Survey Water Resource Investigations Report, Prepared in cooperation with the Mojave Water Agency.

- Van Heeswijk, M. and Smith, D.T., 2002. Simulation of the Ground Water Flow System at Naval Submarine Base Bangor and vicinity, Kitsap County, Washington. US Geological Survey, Water Resources Investigation Report, 02-4261. 142 pp.
- Viruete, J.E., Carbonel, R.I., Martí, D. and Perez-Estaun, A., 2003. 3-D stochastic modeling and simulation of fault zones in the Albala granitic pluton, SW Iberian Variscan Massif. *Journal of Structural Geology*, 25, pp. 1487-1506.
- Water Science and Technology Board, 1990. Groundwater models: Scientific and regulatory application. National Academy Press, Washington DC.
- Xue, Y.Q., 1986. Groundwater Dynamics (in Chinese). Geological Press, China, 227 pp.
- Young, S.R., 1992. The influence of geologic structure on the flow pattern of groundwater in the vicinity of Yuca Mountain – Progress on review of selected literature. Prepared for the Nuclear Regular Commission, San Antonio, Texas.
- Zhang, X., Sanderson, D.J. and Barker, A.J., 2002. Numerical study of fluid flow of deforming fractured rocks using a dual permeability model. *Geophysical Journal International*, 151, pp. 452-468.

APPENDIX 1 DATA OF STEP DRAWDOWN TEST, OCTOBER 2013

GERRITSEN DRILLING SA

OPERATOR: **GEYONDEN FARM** DATE: **14/10/2013**
 LOCATION OF BOREHOLE: **33. 71790 (°S) LATITUDE** SIGNED:
 GPS CO-ORDINATES: **19. 24696 (°E) LONGITUDE**

CALIBRATION DISCHARGE TEST & RECOVERY											
DISCHARGE RATE 1			DISCHARGE RATE 2			DISCHARGE RATE 3			DISCHARGE RATE 3		
DATE & TIME		YIELD	DATE & TIME		YIELD	DATE & TIME		YIELD	DATE & TIME		YIELD
TIME [min]	DRAWDOWN [m]	[l/s]	TIME [min]	DRAWDOWN [m]	(l/s)	TIME [min]	DRAWDOWN [m]	(l/s)	TIME [min]	DRAWDOWN [m]	(l/s)
1	4.90	7.62	1	9.47		1	18.22		1	18.22	
2	6.02		2	10.15	4.10	2	19.18		2	19.18	
3	6.65		3	10.78	5.74	3	19.03	8.16	3	19.03	8.16
5	6.23	4.53	5	12.03	6.04	5	21.01	9.09	5	21.01	9.09
7	5.98	3.40	7	12.13		7	22.06		7	22.06	
10	6.23		10	12.93		10	23.05		10	23.05	
15	6.74		15	13.50		15	23.86		15	23.86	
20	7.18		20	13.97		20	24.55		20	24.55	
30	7.83		30	14.67		30	25.55		30	25.55	
40	8.29		40	15.14		40	26.20		40	26.20	
50	8.68	3.40	50	15.50	6.04	50	26.79	9.09	50	26.79	9.09
60	9.03		60	15.84		60	27.12		60	27.12	

Impact Fault Structure on the Occurrence of Groundwater in Fractured Rock Aquifers

70	80	90	100	110	120	150	180	210	70	80	90	100	110	120	150	180	210	70	80	90	100	110	120	150	180	210
<p>AVERAGE YIELD (l/s) :</p> <p>DRAWDOWN (%) :</p>																										
AVERAGE YIELD (l/s) :									AVERAGE YIELD (l/s) :									AVERAGE YIELD (l/s) :								
DRAWDOWN (%) :									DRAWDOWN (%) :									DRAWDOWN (%) :								

Impact Fault Structure on the Occurrence of Groundwater in Fractured Rock Aquifers

DISCHARGE RATE 4			DISCHARGE RATE 5			DISCHARGE RATE 6		
DATE & TIME			DATE & TIME			DATE & TIME		
TIME [min]	DRAWDOWN [m]	YIELD [l/s]	TIME [min]	DRAWDOWN [m]	YIELD [l/s]	TIME [min]	DRAWDOWN [m]	YIELD [l/s]
1	30.45		1	37.71		1	36.25	
2	32.39	14.98	2	38.10	12.94	2	33.91	
3	32.10	11.58	3	38.50		3	31.28	
5	32.65	12.31	5	39.02	13.71	5	28.22	
7	33.65	12.15	7	40.30	14.12	7	25.42	
10	33.86		10	41.96		10	23.00	
15	34.65		15	42.83		15	20.18	
20	35.03		20	43.77		20	18.21	
30	35.31		30	44.75		30	15.34	
40	35.66		40	45.61		40	13.34	
50	35.98	12.15	50	46.85	14.12	50	12.12	
60	36.42		60	47.05		60	10.99	
70			70			70	10.10	
80			80			80	9.39	
90			90			90	8.75	
100			100			100	8.22	
110			110			110	7.75	
120			120			120	7.28	
150			150			150	6.41	
180			180			180	5.36	
210			210			210	4.27	
240			240			240	3.81	
300			300			300	2.79	
360			360			360		
AVERAGE YIELD (l/s) :			AVERAGE YIELD (l/s) :			AVERAGE YIELD (l/s) :		
DRAWDOWN (%) :			DRAWDOWN (%) :			DRAWDOWN (%) :		

Impact Fault Structure on the Occurrence of Groundwater in Fractured Rock Aquifers

480	17.91	6.06	480	2.67	480	480	480	480	4.66	2.32	480	11.16	1.90
540	18.53		540	2.37	540	540	540	540	5.34	2.03	540	11.70	1.50
600	18.81		600	2.11	600	600	600	600	5.65	1.75	600	12.09	1.18
720	20.07	6.06	720	1.75	720	720	720	720	6.41	1.29	720	12.98	0.83
840	21.74		840	1.43	840	840	840	840	6.78	0.89	840	13.68	0.56
960	22.91		960	1.10	960	960	960	960	7.21	0.53	960	13.98	0.21
1080	23.31	6.03	1080	0.81	1080	1080	1080	1080	7.58	0.29	1080	14.77	0.00
1200	23.73		1200	0.68	1200	1200	1200	1200	8.01	0.05	1200	15.63	
1320	24.11	6.03	1320	0.57	1320	1320	1320	1320	8.42	0.00	1320	16.60	
1440	24.47		1440	0.47	1440	1440	1440	1440	8.88		1440	17.25	
1560			1560		1560	1560	1560	1560			1560		
1680			1680		1680	1680	1680	1680			1680		
1800			1800		1800	1800	1800	1800			1800		
1920			1920		1920	1920	1920	1920			1920		
2040			2040		2040	2040	2040	2040			2040		
2160			2160		2160	2160	2160	2160			2160		
2280			2280		2280	2280	2280	2280			2280		
2400			2400		2400	2400	2400	2400			2400		
2520			2520		2520	2520	2520	2520			2520		
2640			2640		2640	2640	2640	2640			2640		
2760			2760		2760	2760	2760	2760			2760		
2880			2880		2880	2880	2880	2880			2880		
3000			3000		3000	3000	3000	3000			3000		
3120			3120		3120	3120	3120	3120			3120		
3240			3240		3240	3240	3240	3240			3240		
3360			3360		3360	3360	3360	3360			3360		
3480			3480		3480	3480	3480	3480			3480		
3600			3600		3600	3600	3600	3600			3600		
3720			3720		3720	3720	3720	3720			3720		
3840			3840		3840	3840	3840	3840			3840		
3960			3960		3960	3960	3960	3960			3960		
4080			4080		4080	4080	4080	4080			4080		
4200			4200		4200	4200	4200	4200			4200		
4320			4320		4320	4320	4320	4320			4320		
DURATION TOTALS [min]			CDT:		RECOVERY:		OBS 1:	OBS 2:	OBS 3:				
DRAWDOWN / RECOVERY [m]			CDT:		RECOVERY:		OBS 1:	OBS 2:	OBS 3:				
DRAWDOWN / RECOVERY [%]			CDT:		RECOVERY:		OBS 1:	OBS 2:	OBS 3:				
AVERAGE YIELD			CDT:		COMMENTS:								
TRAVELING FOR VERIFICATION [km]				SAMPLE TRANSPORTATION [km]:		GENERAL ITEMS AND MAINTENANCE		TRANSPORT EXISTING EQUIPMENT[km]					

APPENDIX 3 DATA OF CONSTANT HEAD TEST AT BOREHOLE BH-1, OCTOBER 2013

initial water level

BH5 1.25mblc
 BH2 0.58abvC
 BH3

BH-1: 75 mm in diameter
 conductive zone: 67.5 m, 95.3m and 213.0 m

BH1 Constant Head		Time		Duration		Flow (l/s)	
Date	time	hour	minute	second	minute		second
2013-10-14	12:44		0.25			9	2.22
	12:45		0.73		0.48	9	2.22
	12:46		1.05		0.32	14	1.43
	12:47		1.42		0.37	14	1.43
	12:48		3.77		2.35	12	1.67
	12:49		4		0.23	12	1.67
	12:50		5		1	12	1.67
	12:52		7		2	13	1.54
	12:55		10		3	11	1.82
	13:00		15		5	12	1.67
	13:15		20		5	11	1.82
	13:27		32		12	12	1.67
	13:30		35		3	13	1.54
	13:35		40		5	14	1.43
	13:40		45		5	16	1.25
	13:45		50		5	14	1.43
	13:50		60		10	14	1.43
	14:00		70		10	14	1.43
	14:10		80		10	15	1.33
	14:20		90		10	16	1.25
	14:32		102		12	17	1.18
	14:45		115		13	17	1.18
15:00		130		15	18	1.11	
15:20		150		20	19	1.05	
15:50		180		30	22	0.91	
16:20		210		30	22	0.91	
2013-10-14							

Impact Fault Structure on the Occurrence of Groundwater in Fractured Rock Aquifers

16:50	240	30	26	0.77
17:50	300	60	39	0.64
18:50	360	60	42	0.60
19:50	420	60	51	0.49
21:50	540	120	69	0.36
23:50	660	120	82	0.30
2013-10-14	780	120	87	0.29
2013-10-15	900	120	90	0.28
1:50	1 020	120	97	0.26
3:50	1 140	120	120	0.21
5:50	1 260	120	124	0.20
7:50	1 380	120	130	0.19
9:50	1 390	10	126	0.20
11:50	1 510	120	129	0.19
12:00	1 630	120	134	0.19
14:00	1 750	120	136	0.18
16:00	1 870	120	144	0.17
18:00	2 290	420	139	0.18
20:00	2 410	120	141	0.18
2013-10-15	2 530	120	147	0.17
2013-10-16	2650	120	149	0.17
4:00				
6:00				
8:00				
10:00				

APPENDIX 4 DATA OF CD PUMPING TEST, BH-3, NOVEMBER 2006

Duration			Water	Time		Drawdown
Hour	Minute	Second	Level Meter	Hr:Min:Sec	Dt, days	Meter
0	0	0	3.28	0:00:00		
0	1	0	4	0:01:00	0:01:00.0	0.720
0	2	0	4.34	0:02:00	0:02:00.0	1.060
0	3	0	4.59	0:03:00	0:03:00.0	1.310
0	4	0	4.77	0:04:00	0:04:00.0	1.490
0	5	0	4.91	0:05:00	0:05:00.0	1.630
0	6	0	5.09	0:06:00	0:06:00.0	1.810
0	7	0	5.16	0:07:00	0:07:00.0	1.880
0	8	0	5.31	0:08:00	0:08:00.0	2.030
0	9	0	5.33	0:09:00	0:09:00.0	2.050
0	10	0	5.42	0:10:00	0:10:00.0	2.140
0	11	0	5.5	0:11:00	0:11:00.0	2.220
0	12	0	5.53	0:12:00	0:12:00.0	2.250
0	13	0	5.68	0:13:00	0:13:00.0	2.400
0	14	0	5.74	0:14:00	0:14:00.0	2.460
0	15	0	5.78	0:15:00	0:15:00.0	2.500
0	16	0	5.78	0:16:00	0:16:00.0	2.500
0	17	0	5.85	0:17:00	0:17:00.0	2.570
0	18	0	5.87	0:18:00	0:18:00.0	2.590
0	19	0	5.94	0:19:00	0:19:00.0	2.660
0	20	0	6.01	0:20:00	0:20:00.0	2.730
0	25	0	6.17	0:25:00	0:25:00.0	2.890
0	30	0	6.3	0:30:00	0:30:00.0	3.020
0	35	0	6.44	0:35:00	0:35:00.0	3.160
0	40	0	6.59	0:40:00	0:40:00.0	3.310
0	45	0	6.67	0:45:00	0:45:00.0	3.390
0	50	0	6.77	0:50:00	0:50:00.0	3.490
0	55	0	6.81	0:55:00	0:55:00.0	3.530
1	0	0	6.96	1:00:00	1:00:00.0	3.680
1	10	0	7	1:10:00	1:10:00.0	3.720
1	15	0	7.12	1:15:00	1:15:00.0	3.840
1	20	0	7.2	1:20:00	1:20:00.0	3.920
1	30	0	7.39	1:30:00	1:30:00.0	4.110
1	35	0	7.38	1:35:00	1:35:00.0	4.100
1	40	0	7.39	1:40:00	1:40:00.0	4.110
1	50	0	7.5	1:50:00	1:50:00.0	4.220
2	0	0	7.54	2:00:00	2:00:00.0	4.260
2	10	0	7.63	2:10:00	2:10:00.0	4.350
2	20	0	7.71	2:20:00	2:20:00.0	4.430
2	30	0	7.8	2:30:00	2:30:00.0	4.520
2	40	0	7.85	2:40:00	2:40:00.0	4.570
2	50	0	7.86	2:50:00	2:50:00.0	4.580
3	0	0	8.01	3:00:00	3:00:00.0	4.730
3	20	0	8.05	3:20:00	3:20:00.0	4.770
3	40	0	8.05	3:40:00	3:40:00.0	4.770
4	0	0	8.19	4:00:00	4:00:00.0	4.910
4	30	0	8.3	4:30:00	4:30:00.0	5.020
5	0	0	8.33	5:00:00	5:00:00.0	5.050
5	30	0	8.43	5:30:00	5:30:00.0	5.150
6	0	0	8.51	6:00:00	6:00:00.0	5.230

	Duration		Water Level	Time		Drawdown
6	40	0	8.6	6:40:00	6:40:00.0	5.320
7	0	0	8.58	7:00:00	7:00:00.0	5.300
8	0	0	8.74	8:00:00	8:00:00.0	5.460
9	0	0	8.86	9:00:00	9:00:00.0	5.580
10	0	0	8.89	10:00:00	10:00:00.0	5.610
11	0	0	9.03	11:00:00	11:00:00.0	5.750
12	0	0	9.1	12:00:00	12:00:00.0	5.820
13	0	0	9.14	13:00:00	13:00:00.0	5.860
15	0	0	9.28	15:00:00	15:00:00.0	6.000
17	16	0	9.3	17:16:00	17:16:00.0	6.020
18	20	0	9.28	18:20:00	18:20:00.0	6.000
20	0	0	9.3	20:00:00	20:00:00.0	6.020
21	40	0	9.42	21:40:00	21:40:00.0	6.140
23	20	0	9.45	23:20:00	23:20:00.0	6.170
24	0	0	9.49	24:00:00	0:00:00.0	6.210